

MULTIPLE MESON PRODUCTION IN
EMULSIONS EXPOSED TO THE BEVATRON BEAM

WILLIAM RUSSELL JOHNSON

Library
U. S. Naval Postgraduate School
Monterey, California

MULTIPLE MESON PRODUCTION
IN EMULSIONS EXPOSED TO THE BEVATRON BEAM

* * * * *

William R. Johnson

MULTIPLE MESON PRODUCTION
IN EMULSIONS EXPOSED TO THE BEVATRON BEAM

by

William Russell Johnson

Leutenant, United States Navy

Submitted in partial fulfillment
of the requirements
for the degree of
MASTER OF SCIENCE

IN

PHYSICS

United States Naval Postgraduate School
Monterey, California

1955

Tesis
165

Library
U. S. Naval Postgraduate School
Monterey, California

This work is accepted as fulfilling
the thesis requirements for the degree of

MASTER OF SCIENCE

IN

PHYSICS

from the

United States Naval Postgraduate School

MULTIPLE MESON PRODUCTION IN EMULSIONS EXPOSED TO THE BEVATRON BEAM

William R. Johnson

Radiation Laboratory, Department of Physics
University of California, Berkeley, California

May 3, 1955

ABSTRACT

Stacks of 600-micron Ilford G.5 stripped emulsions have been exposed to the internal beam of the Bevatron at three energies: 3.2, 4.8, and 5.7 Bev. Shower-particle production has been investigated at these energies. (A shower particle is defined as one whose grain density is less than 1.4 times minimum.) At each energy 114 events which had beam protons for primaries were found by area scanning. The average shower-particle multiplicities per event were found to be 0.94 ± 0.09 , 1.30 ± 0.11 , and 1.62 ± 0.11 . These results are compared with similar observations by cosmic-ray workers. The various theories of meson production are reviewed and Fermi's calculations for Cosmotron energies have been extended to the energies of this experiment. Production differences in heavy and light nuclei are discussed and compared.

[illegible]

2. 2. 4. 1.

PREFACE

Multiple meson production has been the subject of several papers in recent years and, in the higher energy ranges, cosmic-ray observations have until recently been the only way to compare theory with experiment. The new high-energy particle accelerators, the Cosmotron and Bevatron, accelerate nuclear particles to energies comparable to those found in cosmic rays, and can be used for experimental investigations of meson production.

One method of investigating the interactions of energetic particles--nuclear emulsion technique--has been greatly expanded recently with the development of electron-sensitive emulsions. Detailed observations can be made on such events as nuclear encounters, decays, and scatterings. Emulsions are a versatile tool of physical research and have been used by workers in many fields. In particular, cosmic-ray investigators have made detailed observations of the number of shower particles resulting from the disintegrations of atoms in the emulsions.

It is the aim of this paper to describe observations made in emulsions exposed to the proton beam of the Bevatron and to discuss the theoretical aspects of the interactions that are believed to occur in nucleon-nucleon collisions. Exposure and development techniques are discussed and results are compared with cosmic-ray work in the same field.

The writer wishes to thank Dr. Warren Chupp for his suggestions concerning the problem and informative discussions during the work and the preparation of this paper. He also wishes to thank Drs. Gerson and Sulamith Goldhaber for the use of emulsions from their stacks and for informative discussions of the problem and this paper, Dr. Edward Milne for his review of this paper, Dr. Joseph V. Lepore for a discussion of his nuclear model, Mr. Joseph Lannutti for his unpublished data on prong distributions and instruction in development techniques, and Mrs. Marjorie Hirsch for help with this manuscript.

This work was carried out under the auspices of the U. S. Atomic

the first of these is the fact that the
the second is the fact that the
the third is the fact that the
the fourth is the fact that the
the fifth is the fact that the
the sixth is the fact that the
the seventh is the fact that the
the eighth is the fact that the
the ninth is the fact that the
the tenth is the fact that the
the eleventh is the fact that the
the twelfth is the fact that the
the thirteenth is the fact that the
the fourteenth is the fact that the
the fifteenth is the fact that the
the sixteenth is the fact that the
the seventeenth is the fact that the
the eighteenth is the fact that the
the nineteenth is the fact that the
the twentieth is the fact that the
the twenty-first is the fact that the
the twenty-second is the fact that the
the twenty-third is the fact that the
the twenty-fourth is the fact that the
the twenty-fifth is the fact that the
the twenty-sixth is the fact that the
the twenty-seventh is the fact that the
the twenty-eighth is the fact that the
the twenty-ninth is the fact that the
the thirtieth is the fact that the
the thirty-first is the fact that the
the thirty-second is the fact that the
the thirty-third is the fact that the
the thirty-fourth is the fact that the
the thirty-fifth is the fact that the
the thirty-sixth is the fact that the
the thirty-seventh is the fact that the
the thirty-eighth is the fact that the
the thirty-ninth is the fact that the
the fortieth is the fact that the
the forty-first is the fact that the
the forty-second is the fact that the
the forty-third is the fact that the
the forty-fourth is the fact that the
the forty-fifth is the fact that the
the forty-sixth is the fact that the
the forty-seventh is the fact that the
the forty-eighth is the fact that the
the forty-ninth is the fact that the
the fiftieth is the fact that the
the fifty-first is the fact that the
the fifty-second is the fact that the
the fifty-third is the fact that the
the fifty-fourth is the fact that the
the fifty-fifth is the fact that the
the fifty-sixth is the fact that the
the fifty-seventh is the fact that the
the fifty-eighth is the fact that the
the fifty-ninth is the fact that the
the sixtieth is the fact that the
the sixty-first is the fact that the
the sixty-second is the fact that the
the sixty-third is the fact that the
the sixty-fourth is the fact that the
the sixty-fifth is the fact that the
the sixty-sixth is the fact that the
the sixty-seventh is the fact that the
the sixty-eighth is the fact that the
the sixty-ninth is the fact that the
the seventieth is the fact that the
the seventy-first is the fact that the
the seventy-second is the fact that the
the seventy-third is the fact that the
the seventy-fourth is the fact that the
the seventy-fifth is the fact that the
the seventy-sixth is the fact that the
the seventy-seventh is the fact that the
the seventy-eighth is the fact that the
the seventy-ninth is the fact that the
the eightieth is the fact that the
the eighty-first is the fact that the
the eighty-second is the fact that the
the eighty-third is the fact that the
the eighty-fourth is the fact that the
the eighty-fifth is the fact that the
the eighty-sixth is the fact that the
the eighty-seventh is the fact that the
the eighty-eighth is the fact that the
the eighty-ninth is the fact that the
the ninetieth is the fact that the
the ninety-first is the fact that the
the ninety-second is the fact that the
the ninety-third is the fact that the
the ninety-fourth is the fact that the
the ninety-fifth is the fact that the
the ninety-sixth is the fact that the
the ninety-seventh is the fact that the
the ninety-eighth is the fact that the
the ninety-ninth is the fact that the
the hundredth is the fact that the

Energy Commission at the Radiation Laboratory of the University of California while the author was assigned there from the U.S. Naval Postgraduate School.

TABLE OF CONTENTS

Item	Title	Page
Chapter I	Introduction	
	1. Nuclear Forces	1
	2. High-Energy Nucleon-Nucleon Encounters .	2
Chapter II	Theories of Meson Production and Star Formation	
	1. General	4
	2. Plural Theory	4
	3. Multiple Theories	5
	4. Star Formation	8
Chapter III	The Bevatron as a Source of High-Energy Protons	
	1. Acceleration of Protons	10
	2. Using the Internal Proton Beam	14
Chapter IV	Nuclear Emulsions--Exposure and Processing	
	1. Nuclear Emulsions	18
	2. Internal Beam Exposure	19
	3. Processing Emulsions	20
Chapter V	Experimental Method	
	1. Experimental Nomenclature and Criteria .	22
	2. Experimental Procedure	23
Chapter VI	Experimental Results	
	1. Yield Curves for \bar{n}_s and \bar{N}_h	25
	2. Shower-Particle Multiplicity	27
	3. Distribution of Star Sizes	30
	4. Comparison of Disintegrations of Light and Heavy Nuclei	33
	5. General Observations	37

Chapter 1

Chapter 1

Chapter 2

Chapter 2

Chapter 3

Chapter 3

Chapter 4

Chapter 4

Chapter 5

Chapter 5

Chapter 6

Chapter 6

Chapter 6

Chapter 6

Chapter 6

Chapter 6

Chapter 6

TABLE OF CONTENTS

Item	Title	Page
Chapter VII (Cont.)	Theoretical Comparisons	
	1. Fermi Model	38
	2. Lepore Model	38
	3. Other Theories	40
	4. General Comment	41

LIST OF ILLUSTRATIONS AND TABLES

Figure		Page
1.	Bevatron Schematic	13
2. a and b	Air Lock and Probe Assemblies	15, 16
3.	Emulsion Stack Mounted on a Probe Head	17
4.	π_s and \bar{N}_h versus Primary Particle Energy	26
5.	Normalized Shower-Particle Multiplicities at 3.2 Bev	28
6.	Normalized Shower-Particle Multiplicities at 4.8 and 5.7 Bev	29
7. a - d	Normalized Prong Distributions	31, 32
8.	\bar{n}_s versus Primary-Particle Energy for Heavy and Light Nuclei ($n_s \geq 0$)	35
9.	\bar{n}_s versus Primary-Particle Energy for Heavy and Light Nuclei ($n_s \geq 1$)	36

Table

I	Bevatron Statistics	12
II	Steps in Bristol Development Method	21
III	Average Number of Prongs per Star	33
IV	Observed and Calculated Shower-Particle Multiplicity Percentages--Fermi Model	39
V	Pion Production at 6.3 Bev--Lepore Model	40
VI	Average Shower-Particle Multiplicities--Heitler and Heisenberg Theories	41

1917

1917

1917

1917

1917

1917

1917

1917

1917

1917

1917

1917

1917

1917

1917

1917

1917

1917

CHAPTER I

INTRODUCTION

1. Nuclear Forces.

The structure of the atomic nucleus and the nature of its binding forces are the foremost problems of the nuclear physicist. In early stages of the studies of nuclear forces it was hoped that the development of nuclear physics would parallel that of atomic physics. Investigations of the smallest atomic unit, the stable hydrogen atom, disclosed the nature of atomic structure and forces. A complete theory substantiated by experimental facts was then evolved. In the study of the smallest unit in which nuclear forces play a part, the deuteron, it has not been possible to accumulate sufficient data to formulate a consistent general theory because there is essentially only one bound state, not the several states found in the structure of the hydrogen atom. The study of larger nuclei introduces the complexities of the many-body problem and therefore a complete analysis in the general case is not possible.

In quantum electrodynamics each particle interacts only with the electromagnetic field. The interaction between two particles is through the field and can be explained in terms of an exchange of discrete energy quanta between the interacting particles. The quanta are the zero-rest-mass photons of the electromagnetic field. Yukawa suggested that forces between nucleons might be due to a similar field, now identified as the meson field. A characteristic difference between nuclear forces and electromagnetic forces is that nuclear forces act only at very short distances (of the order of 10^{-13} cm), whereas the electromagnetic forces have no characteristic length.

The range R of nuclear forces is the maximum distance at which two nucleons can interact as a result of one particles emitting a virtual meson which is then absorbed by the other. If this virtual meson travels with the velocity of light, it exists for a time

$$\Delta t = R/c.$$

The first part of the paper is devoted to a discussion of the experimental results obtained in the study of the photoelectric effect. The results show that the photoelectric effect is a quantum phenomenon, and that the energy of the incident light must be greater than the work function of the metal in order for electrons to be emitted. The second part of the paper is devoted to a discussion of the theory of the photoelectric effect. The theory is based on the assumption that the energy of the incident light is quantized, and that the energy of the emitted electrons is equal to the energy of the incident light minus the work function of the metal. The third part of the paper is devoted to a discussion of the experimental results obtained in the study of the photoelectric effect. The results show that the photoelectric effect is a quantum phenomenon, and that the energy of the incident light must be greater than the work function of the metal in order for electrons to be emitted. The fourth part of the paper is devoted to a discussion of the theory of the photoelectric effect. The theory is based on the assumption that the energy of the incident light is quantized, and that the energy of the emitted electrons is equal to the energy of the incident light minus the work function of the metal. The fifth part of the paper is devoted to a discussion of the experimental results obtained in the study of the photoelectric effect. The results show that the photoelectric effect is a quantum phenomenon, and that the energy of the incident light must be greater than the work function of the metal in order for electrons to be emitted.

The first part of the paper is devoted to a discussion of the experimental results obtained in the study of the photoelectric effect. The results show that the photoelectric effect is a quantum phenomenon, and that the energy of the incident light must be greater than the work function of the metal in order for electrons to be emitted. The second part of the paper is devoted to a discussion of the theory of the photoelectric effect. The theory is based on the assumption that the energy of the incident light is quantized, and that the energy of the emitted electrons is equal to the energy of the incident light minus the work function of the metal. The third part of the paper is devoted to a discussion of the experimental results obtained in the study of the photoelectric effect. The results show that the photoelectric effect is a quantum phenomenon, and that the energy of the incident light must be greater than the work function of the metal in order for electrons to be emitted. The fourth part of the paper is devoted to a discussion of the theory of the photoelectric effect. The theory is based on the assumption that the energy of the incident light is quantized, and that the energy of the emitted electrons is equal to the energy of the incident light minus the work function of the metal. The fifth part of the paper is devoted to a discussion of the experimental results obtained in the study of the photoelectric effect. The results show that the photoelectric effect is a quantum phenomenon, and that the energy of the incident light must be greater than the work function of the metal in order for electrons to be emitted.

During the existence of the meson the energy of the system is increased by

$$\Delta E = m_{\pi} c^2.$$

This, however, is a violation of the energy conservation law and by the uncertainty principle the violation can exist for only a time consistent with the uncertainty of measurement

$$\hbar = \Delta E \cdot \Delta t = m_{\pi} c R.$$

Therefore the mass of the meson field quantum is

$$m_{\pi} = \hbar / Rc = 300 \text{ electron mass units.}$$

This quantum is analogous to the photon of the electromagnetic field.

When the wave-particle dualism of nature is considered, quanta can be regarded as waves that can be emitted from the nucleus. The waves are concentrated within the nuclear volume and their constructive interference represents particle emission. These quanta, pions, are thought to be the building blocks of nuclear matter, and are the source of difficulties that arise when attempts are made to formulate a nuclear theory along the same lines as the electromagnetic theory. Wave lengths of pions are much shorter than those of most photons, so that higher energies are required for the perturbing particles. When higher energies are used, the creation of mesons introduces a many-body problem and complicates field-theory predictions.

2. High-Energy Nucleon-Nucleon Encounters.

The domains involved in the investigations of nuclear forces are so small that answers must be derived indirectly from observations of events that occur when a nucleus is perturbed by a high-energy particle. Cloud chambers and the various types of fast electronic counters had been the principal instruments for the study of nuclear forces prior to the development of sensitive nuclear emulsions. High-energy particle accelerators and cosmic rays have been used as sources of primary nucleons to strike target nuclei in emulsions. The incident nucleon, in the Bev range, makes one or several collisions with the individual nucleons of the nucleus within 10^{-23} second. This time is approxi-

mately that required for a particle traveling with the speed of light to traverse the nucleus. Compared with the period of motion of nucleons the collision time is short, because of the short DeBroglie wave length of the incident particle. The short wave length localizes the particle to a small region in space and makes encounters with individual nucleons possible. In effect, there is a series of collisions or a cascade process within the nuclear volume which may be radiative or elastic. In radiative collisions various types of quanta (mesons) may be radiated. In both types of collisions recoil nucleons are produced, which may either escape immediately or interact further with other nucleons (and may subsequently escape after having undergone one or more encounters).

Studies of collision processes can be approached in different ways. Each approach will add to the store of physical knowledge and the final results may contain explanations for the many unanswered questions. One phase of the problem is the process of meson production and its variation with incoming particle energy. Theories have been developed to the extent that direct comparison with experiment can be made. Cosmic-ray workers have investigated production in nucleon-nucleon collisions and, with the advent of the high-energy proton-synchrotrons at Brookhaven and Berkeley, physicists have begun similar investigations using pure proton beams.

This paper is concerned with multiple meson production by protons in the Bev range and includes the following aspects of the problem: the theoretical proposals that have been advanced to explain the processes involved, the use of the Bevatron and nuclear emulsions to produce and detect mesons, the results of a detailed study of meson production, and a comparison of these results with theoretical predictions and observations made on production from cosmic rays. This study represents an addition to previous work because pure proton beams at known Bev energies were used whereas previous investigations were carried out with primaries that were an admixture of protons and pions.

CHAPTER II

THEORIES OF MESON PRODUCTION AND STAR FORMATION

1. General.

Theories relating to meson production in high-energy nucleon-nucleon collisions may be divided into two general classes, plural and multiple. Fundamentally these two theories differ in principle. In the plural theory of Heitler and Janossy [13, 14] the radiation-damping effect is assumed to be so strong that only a single meson can be produced per collision in the majority of cases. This assumption is postulated on the basis of the strong meson coupling of the Yukawa theory. The coupling is so postulated that a single meson can be emitted if the energy is supplied and is of the proper order of magnitude to account for the nuclear forces. The multiple theories of Heisenberg [12], Lewis et al. [19], Fermi [5], and Lepore [18] assume that several mesons can be created in a single collision so inelastic that the primary does not have sufficient energy to create more mesons. In a large nucleus when there is enough energy available both theories predict a meson shower and differences can not be noted. On the other hand, when a nucleus of low atomic mass number is struck, very different results are predicted.

2. Plural Theory.

In the pure form of the plural theory Heitler and Janossy assumed (a) in each nucleon-nucleon collision only one meson is produced, (b) the mean free path for a collision is of the order of the internucleon distance, and (c) the nucleus is completely transparent to the created mesons and recoil nucleons. The total plurality is then given by the number of encounters that the primary nucleon makes in passing through the nucleus.

In each collision the primary loses a fraction σ of its kinetic energy; of this, the recoil nucleon takes a fraction α and the created meson is left with the remainder $\sigma - \alpha$. There is a definite cutoff energy below which meson production ceases. After n meson-pro-

ducing collisions, the primary has an energy of $(1-\sigma)^n E_0$ and n recoil nucleons have been produced with energies of $(1-\sigma)^{n-1} E_0$. As long as the primary energy is greater than the cutoff energy more mesons will be created. From these considerations Heitler estimates the total number of charged and neutral mesons created to be

$$N_s = \frac{\log(\gamma_p - 1) - \log(\gamma_c - 1) + 1}{-\log(1-\sigma)}, \quad (1)$$

where γ_p is the primary energy in rest mass units, γ_c is cutoff energy in the same units. When only those mesons with kinetic energy greater than 80 Mev are considered, γ_c equals 3.1. Heitler assumed $\sigma = 0.25$ and $\alpha = 0.125$. If there is symmetrical charge distribution in mesons, two-thirds of the created mesons must be charged.

Heitler's theory appears to give reasonable results except at high primary energies, where the recoil nucleons and created mesons have energies above the meson-production threshold. These particles could themselves act as primaries in generating more mesons. In the modified plural theory the same authors included the possibilities of production by second and higher generations.

3. Multiple Theories.

The multiple theories start with the assumption of possible production of more than one meson per collision, and take into account the opacity of the nucleus to the created mesons. The various theoreticians use different approaches, however, in analyzing the collisions.

Lewis et al. use the problem of electromagnetic radiation as an analogy and make assumptions that (a) collision time is short compared to periods of emitted radiation, (b) effects of the emitted radiation, particularly its recoil, may be neglected, and (c) components of the radiation field for which these considerations are satisfied are the only ones that need be considered. When these conditions are fulfilled, the radiated spectrum is the difference between the quasi-static field of the radiator before collision and the field after colli-

the first of these is the fact that the
the second is the fact that the
the third is the fact that the
the fourth is the fact that the
the fifth is the fact that the
the sixth is the fact that the
the seventh is the fact that the
the eighth is the fact that the
the ninth is the fact that the
the tenth is the fact that the
the eleventh is the fact that the
the twelfth is the fact that the
the thirteenth is the fact that the
the fourteenth is the fact that the
the fifteenth is the fact that the
the sixteenth is the fact that the
the seventeenth is the fact that the
the eighteenth is the fact that the
the nineteenth is the fact that the
the twentieth is the fact that the
the twenty-first is the fact that the
the twenty-second is the fact that the
the twenty-third is the fact that the
the twenty-fourth is the fact that the
the twenty-fifth is the fact that the
the twenty-sixth is the fact that the
the twenty-seventh is the fact that the
the twenty-eighth is the fact that the
the twenty-ninth is the fact that the
the thirtieth is the fact that the
the thirty-first is the fact that the
the thirty-second is the fact that the
the thirty-third is the fact that the
the thirty-fourth is the fact that the
the thirty-fifth is the fact that the
the thirty-sixth is the fact that the
the thirty-seventh is the fact that the
the thirty-eighth is the fact that the
the thirty-ninth is the fact that the
the fortieth is the fact that the
the forty-first is the fact that the
the forty-second is the fact that the
the forty-third is the fact that the
the forty-fourth is the fact that the
the forty-fifth is the fact that the
the forty-sixth is the fact that the
the forty-seventh is the fact that the
the forty-eighth is the fact that the
the forty-ninth is the fact that the
the fiftieth is the fact that the
the fifty-first is the fact that the
the fifty-second is the fact that the
the fifty-third is the fact that the
the fifty-fourth is the fact that the
the fifty-fifth is the fact that the
the fifty-sixth is the fact that the
the fifty-seventh is the fact that the
the fifty-eighth is the fact that the
the fifty-ninth is the fact that the
the sixtieth is the fact that the
the sixty-first is the fact that the
the sixty-second is the fact that the
the sixty-third is the fact that the
the sixty-fourth is the fact that the
the sixty-fifth is the fact that the
the sixty-sixth is the fact that the
the sixty-seventh is the fact that the
the sixty-eighth is the fact that the
the sixty-ninth is the fact that the
the seventieth is the fact that the
the seventy-first is the fact that the
the seventy-second is the fact that the
the seventy-third is the fact that the
the seventy-fourth is the fact that the
the seventy-fifth is the fact that the
the seventy-sixth is the fact that the
the seventy-seventh is the fact that the
the seventy-eighth is the fact that the
the seventy-ninth is the fact that the
the eightieth is the fact that the
the eighty-first is the fact that the
the eighty-second is the fact that the
the eighty-third is the fact that the
the eighty-fourth is the fact that the
the eighty-fifth is the fact that the
the eighty-sixth is the fact that the
the eighty-seventh is the fact that the
the eighty-eighth is the fact that the
the eighty-ninth is the fact that the
the ninetieth is the fact that the
the ninety-first is the fact that the
the ninety-second is the fact that the
the ninety-third is the fact that the
the ninety-fourth is the fact that the
the ninety-fifth is the fact that the
the ninety-sixth is the fact that the
the ninety-seventh is the fact that the
the ninety-eighth is the fact that the
the ninety-ninth is the fact that the
the hundredth is the fact that the

sion. The conditions apply to the most intense fields closest to the nucleons, therefore the collision problem can be considered only for primary energies greater than 100 Bev. In effect, the emission mechanism is very similar to that in the case of ordinary bremsstrahlung, where the radiated electromagnetic field can be thought of as the difference between the quasi-static field of the incident electron and that of the scattered electron.

Heisenberg describes a high-energy collision by assuming that the pion fluid surrounding the nucleus is set into motion by the impact energy. In order to estimate energy distribution he uses qualitative ideas of turbulence; these ideas represent an approach to thermal equilibrium in a fluid. Spreading of the energy of motion into many states of larger and larger wave number is postulated. The total number of mesons produced will then vary with primary energy and inelasticity of the collision. The inelasticity K is defined as the ratio of the energy radiated as mesons in the center-of-mass system to the maximum amount of energy available in this system.

The value of K does not come directly from the theory. At high primary energies the mean value of K must be near unity, according to considerations of equipartition of momentum between nucleons and pions. In the lower energy regions K varies with energy and its value must be determined experimentally.

Fermi goes one step further than Heisenberg and assumes that statistical¹ equilibrium has been reached before mesons are emitted because the interactions taking part in meson production are so strong. According to Fermi, when two nucleons collide with high center-of-mass energies, the energy is localized in a small volume surrounding the nucleons. This spherical volume for interaction has a radius equal to the meson Compton wave length, $\hbar/m_{\pi}c$, and is flattened in the direction of motion by the Lorentz contraction. Since statistical equilibrium is reached in this volume, the number of states available to the e-

1. See Milburn [22] for a review article on statistical meson production theories.

mitted particles in phase space can be calculated from the principles of statistical mechanics and thereby one can determine the relative multiplicity and momentum distributions.

Fermi has calculated statistical weights for each state dependent upon charge distributions, but neglected interference effects and angular momentum states. Nucleons are treated as nonrelativistic and pions as very relativistic, and momentum is not conserved among pions. His results give the relative probability for the production of n mesons as a function of energy,

$$f_n(w) = \frac{\left[\frac{251}{w} (w-2)^3 \right]^n}{\left[\frac{3}{2} \times \frac{5}{2} \cdots \frac{6n-1}{2} \right]}, \quad (2)$$

where w is the total energy of the colliding nucleons in the center-of-mass system in units of nucleon rest energy.

Fermi supplemented his original paper with a paper on pion production at Cosmotron energies [6], in which he considered the effects of charge conservation for the nucleons and pions, a consideration neglected in the earlier theory. He made computations for low-multiplicity production--three pions or less. The number of possible types of transitions was restricted by requiring that isotopic spin be conserved. For any statistical consideration of a high-energy collision, all final states are formed with a probability proportional to the weight of that state, providing it can be reached from the ground state without violating the laws of conservation of energy, momentum, angular momentum, charge, and isotopic spin. Fermi's calculations for Cosmotron energies can be extended to Bevatron energies to give multiplicities expected in the experiment, so a rather complete discussion follows.

The initial state before a collision of two nucleons may have either isotopic spin $T = 1$ or $T = 0$; consequently, only those final states with isotopic spin one or zero need be considered. Each state has a number of charge possibilities. After Fermi, let p_n be the number of possibilities for $T = 1$ and q_n be the number of possibilities for $T = 0$.

In a collision of two protons the initial isotopic spin state is

$T = 1$; therefore the most abundant final state will be the same. Its probability will be proportional to f_n (from Eq. (2)) and p_n . In a collision between a proton and neutron the initial states are $T = 1$ and $T = 0$, so the final states will also be $T = 1$ and $T = 0$. For $T = 0$ the probability would be as above, substituting q_n for p_n . The resultant final probability is an average of the two. Expressions have the following form:

$$P_n = p_n f_n / \sum p_n f_n, \quad Q_n = p_n q_n / \sum q_n f_n. \quad (3)$$

The charges of the pions, as well as their multiplicity, must be known before the above figures can be compared with experiment, because only charged mesons can be observed directly. The number of neutrals must be subtracted from the theoretical values before comparison can be made. The numbers p_n and q_n may be subdivided into states corresponding to possible charges and their weights can be determined. These values are tabulated by Fermi for p-p and p-n collisions and are used in calculations of the multiplicities given in Table IV, Chapter VII.

Lepore has used a statistical model and followed Fermi in assuming the establishment of a state approximating equilibrium before meson emission. Probability of disintegration into the various possible modes is proportional to a relative extension of accessible phase space. His interaction volume does not have the Lorentz contraction of the Fermi model, but he obtains what might be considered a uniform shrinkage of the configurational volume with increasing energy by energy-dependent cutoffs.

4. Star Formation.

In the theoretical aspects of a collision considered in the earlier sections only the mechanisms responsible for meson formation have been discussed. This is the initial step in star formation and takes place in 10^{-23} second. The complete nuclear disintegration involves emission of a few particles which may include the primary nucleon, knock-on nucleons and created mesons, and a number of slow particles with an average energy of 10 Mev. If the energy distributions were

plotted, there would not be a break between the two groups, but the first group would appear as a high-energy tail on the second.

The slow particles arise as a result of the nuclear excitation by the fast particles of the first group, and their emission is analogous to evaporation. The evaporation theory as first postulated by Bohr was extended by Harding et al. [17] to low-energy particles from stars. They found, using the Fermi gas model of the nucleus and making allowance for cooling and barrier penetration, that the theory made reasonable predictions of the observed energy spectrum. Using a nuclear model with mass near 100, LeCouteur [17] extended Harding's work by taking into account the thermal expansion and the neutron excess of the residual nucleus. He obtained energy distributions of evaporated particles and calculated probabilities for emission of protons, neutrons, deuterons, tritons, He^3 , and alpha particles as a function of excitation energy. The assumption that the nucleus always remains in an approximate state of thermal equilibrium requires that excitation energies be less than 600 Mev, thereby restricting the validity of the calculations to a maximum star size of about fourteen prongs. Since the light nuclei were excluded in the basic model, LeCouteur's theory is strictly applicable only to stars having between six and fourteen prongs.

Fujimoto and Yamaguchi [8,9] have considered the same problem, taking into account the changes in binding energy of nuclear particles during evaporation. They envisage a step-by-step process in which thermal equilibrium is reached between each particle emission.

The general mechanism as postulated by all workers is that the excitation energy results from the kinetic energy of nucleons that have undergone collisions but do not have enough energy to escape immediately. The kinetic energy distributes itself statistically, raising the nuclear "temperature" as a whole and causing evaporation. It is estimated that the evaporation processes occur within approximately 10^{-16} second after the collision.

CHAPTER III

THE BEVATRON AS A SOURCE OF HIGH-ENERGY PROTONS

1. Acceleration of Protons.

In order to investigate disintegrations resulting from high-energy nucleon-nucleon interactions, balloons have been flown with emulsions and cloud chambers into the upper atmosphere where there is a flux of very energetic pions and nucleons. High-energy accelerators have been developed to provide intense controlled particle beams at energies comparable to median values found in cosmic rays. In this experiment the Berkeley Bevatron has been used as a source of energetic protons. A short discussion of its characteristics is appropriate.

The Bevatron is a proton synchrotron which utilizes the principle of "phase stability" as evolved by Veksler and McMillan. (Bohm and Foldy discuss this principle in detail in their article on "Theory of the Synchrotron" [24].) The angular velocity of a particle with a charge e and relativistic mass m in a magnetic field H is given by

$$\omega = eH/mc = ecH/E \quad (4)$$

The phase-stable particle will stay in or near its stable orbit even though small disturbing forces are applied to it. This implies that the acceleration can be accomplished by slowly varying the magnetic and electric fields.

Equation (4) can be rewritten in the following form:

$$cp/eH = r = \text{constant for a synchrotron.} \quad (5)$$

Equation (5) then represents the relationship between momentum and magnetic field necessary in order to keep a particle in its orbit. Differentiation of Eq. (5) gives the relation between the incremental values:

$$\Delta p/p = \Delta H/H. \quad (6)$$

The particle orbit is stable and will follow any slow, or adiabatic, variation of the magnetic field with time in which $\Delta H/H \ll 1/\omega$. In order to provide focusing forces as well as satisfy conditions for phase stability, the magnetic field must be designed with the proper spatial variation. This variation is expressed by the logarithmic field index n .

$$H = H_0 \left[r/r_0 \right]^{-n} \quad \text{or} \quad n = - \left[r/H \cdot dH/dr \right] ; \quad 0 < n < 1 \quad n \neq 0.5. \quad (7)$$

The particle will not remain exactly in the orbit described by Eq. (5), but will execute slow variations about it. The variations are a function of n and ω , and their amplitude varies inversely with the square root of the magnetic field [15, 16] .

The theoretical aspects of charged-particle motion discussed in the previous paragraphs establish the basic requirements for a proton synchrotron: a means of supplying energy to a particle in small steps and a means of guiding it over the path to be followed while gaining energy. The first is done by keeping the accelerating system in an orbital path which the particle uses many times. The second is obtained by having a circular magnet wherein the field decreases with increasing radius. The particle can have its energy increased by changing the frequency and field as indicated by Eq. (4). With the machine radius selected as a design constant, Eq. (5) shows that maximum momentum (or energy) is a function of the field obtainable. The field maximum is limited by such design considerations as magnet size, aperture, and cost.

In the Bevatron the particle trajectory is through four annular quadrants which comprise the magnet. The quadrants are connected by four straight sections which serve to give a field-free space for location of the accelerating electrode, proton injector, vacuum pumps, targets, etc.

Figure 1 is a schematic representation of the Bevatron, showing dimensions and relative locations of the major components. Table I gives Bevatron Statistics.

Table I

Bevatron Statistics

Radius of equilibrium orbit	50 ft.
Length of straight sections	20 ft.
Size of beam aperture	1 ft. by 4 ft.
Injection energy	9.8 Mev
Maximum final energy	6.3 Bev
Initial accelerating frequency	~ 356 kc
Final accelerating frequency	$\sim 2,500$ kc
Initial field	~ 300 gauss
Peak field	$\sim 15,870$ gauss
Magnet cycle	6 sec
Field index	$0.53 < n < 0.73$
Accelerating time (rising magnetic field)	1.75 sec
Repetition rate	6 pulses/min
Energy gain/turn	1.5 kev
No. of protons injected	$\sim 10^{13}$
No. of protons reaching maximum energy (a)	$\sim 10^{10}$
Beam cross section after injection	1 ft. by 4 ft.
Final beam cross section	~ 1.5 in. by 4 in.
Operating pressure	10^{-5} mm Hg
Peak magnet power	100,000 kva

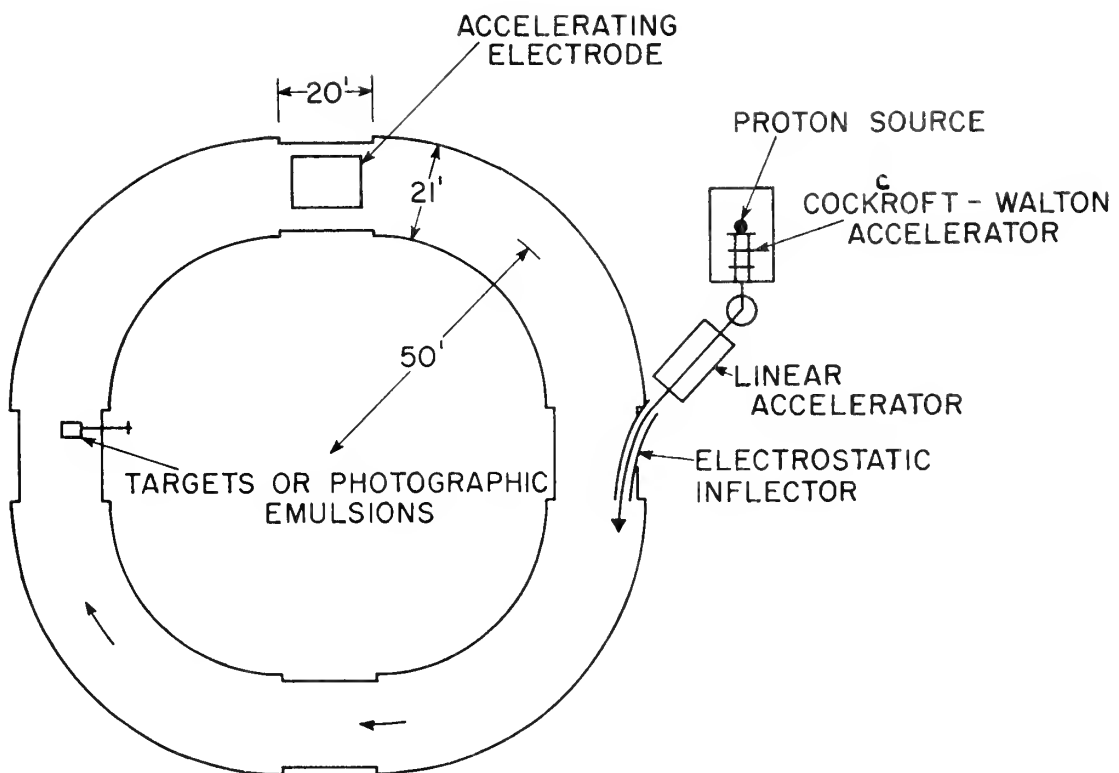
a - The beam intensity is reduced for emulsion exposures in the internal beam.

Protons must be injected at the proper energy and radial position commensurate with the initial field and accelerating frequency in order to stay within the annular magnet sections. After injection H and ω are increased until the particle reaches desired energy. The desired energy can be chosen by the selection of an acceleration (rf) field turn-off time. After rf turnoff H continues to increase, causing the equilibrium orbit to shrink. The next sequence of events depends on the desired use of the beam.

1

1. *Phragmites* (Common Reed)

Dated at London this 27th day of May 1968



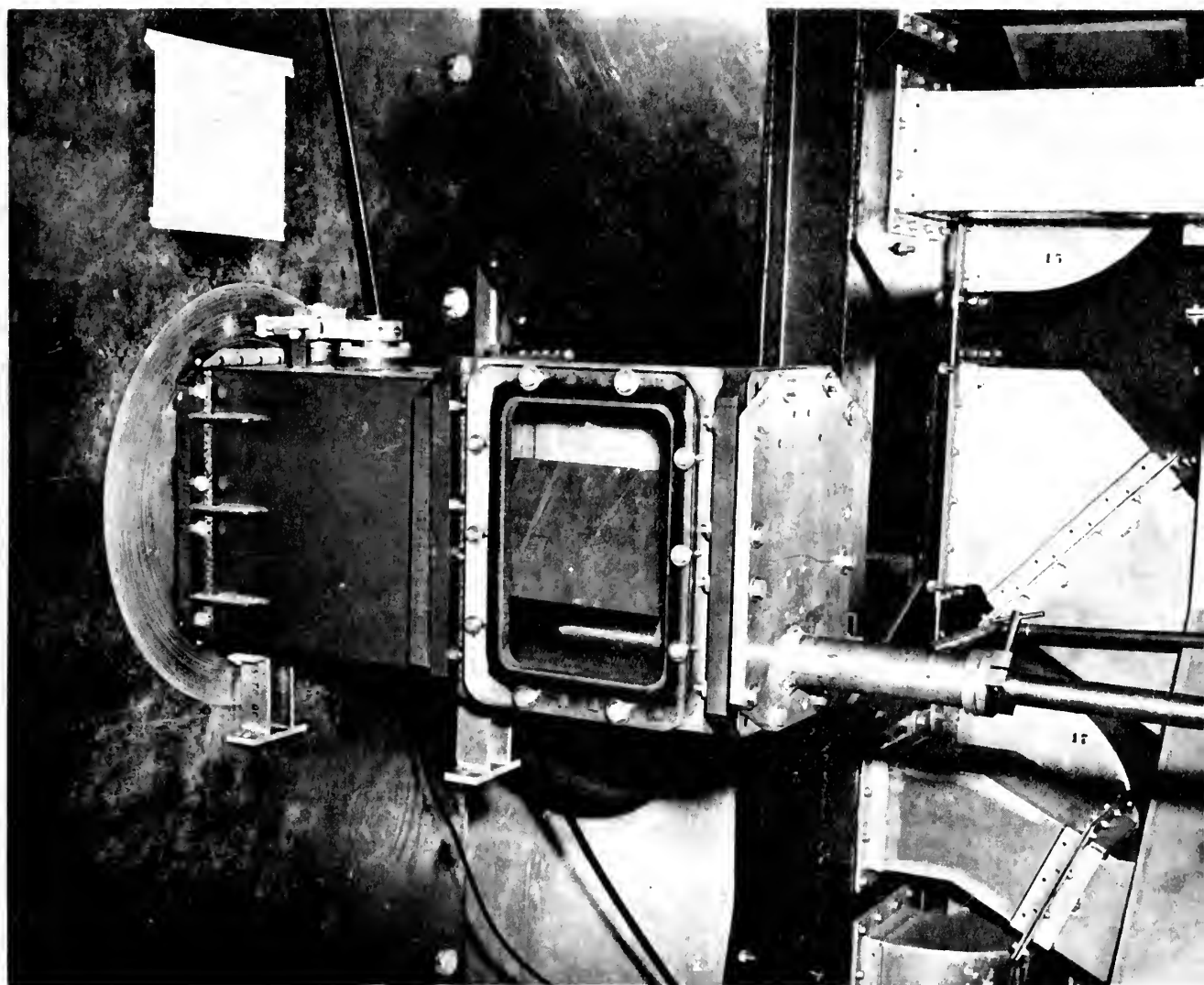
MU-9294

Fig. 1. Schematic of the Bevatron

2. Using the Internal Proton Beam.

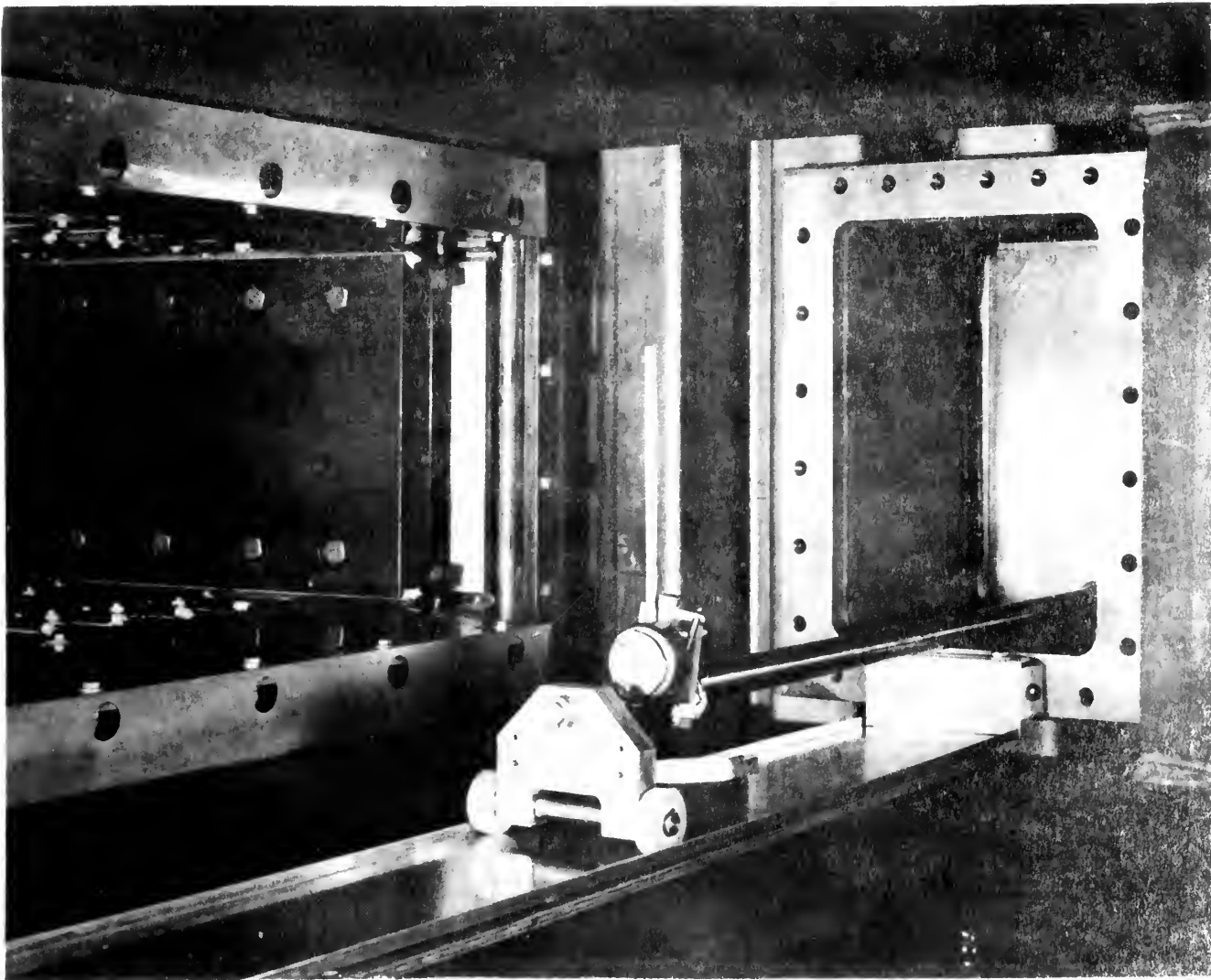
Internal exposures in the vacuum system were made in this experiment by direct bombardment of emulsion targets or allowing the beam to penetrate a lip target extending one or two centimeters from the edge of the emulsion stack. The lip serves to damp out radial oscillations and increase the spacing between successive passages of the beam. The internal beam is also used for external exposures by putting a target into the beam and observing secondary particles created. Thin windows are located so the target can be viewed from various detector stations where analyzing magnets and collimated beams can be used for charge, mass, and momentum selection.

The inner radial surface of one straight section is fitted with air locks to facilitate internal exposures and bombardments. A small air lock with a 6-by-13-inch aperture has a probe mounted in it without an internal support. Loads up to ten pounds are plunged into the beam orbit on this probe. A larger air lock with an 18-by-20-inch aperture is used for loads up to 150 pounds. With this lock and its associated probe mechanism, targets can be mounted on a trolley car which travels into the vacuum system on support rails. Figure 2a is a photograph of a small type air lock and part of its probe assembly. Figure 2b is a photograph from the inside of a straight section showing a probe with a trolley and support rails. Figure 3 is a photograph of a test emulsion stack mounted on a probe. The piece of lucite taped on the end is the lip referred to above.



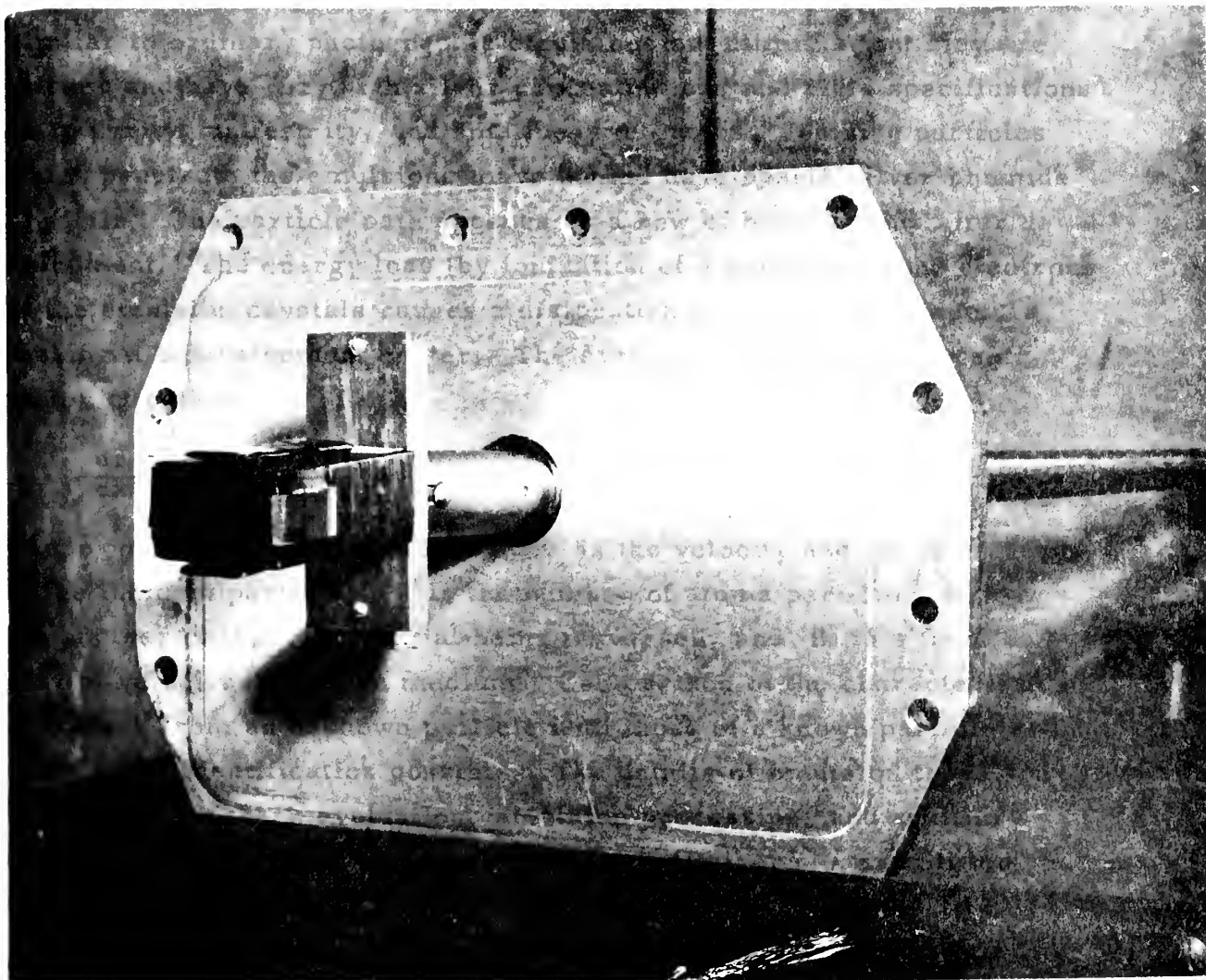
ZN-1224

Fig. 2a. Air lock and probe on inner radial wall of west straight section of Bevatron.



ZN-1223

Fig. 2b. Internal view of west straight section showing a flip-up target mounted on a probe with an internal support.



ZN-1225

Fig. 3. Stack of 2-inch by 4-inch 600-micron emulsion pellicles mounted on a Bevatron probe used for internal beam exposures.



CHAPTER IV

NUCLEAR EMULSIONS - EXPOSURE AND PROCESSING

1. Nuclear Emulsions.

The recent development of nuclear emulsions that are sensitive to all charged particles has provided researchers with an excellent quantitative as well as qualitative research tool. Nuclear emulsions are similar to ordinary photographic emulsions but differ in that they are thicker and have very high silver concentrations and rigid specifications as to purity, uniformity, and smallness of grains. Ionizing particles which penetrate the emulsions leave behind developable silver bromide crystals. The particle path appears as a row of black grains after development. The energy loss (by ionization of a particle) to the electrons of the emulsion crystals causes a dislocation in the crystal structure, making it a development center. The average energy loss per centimeter of path is

$$-\frac{dE}{dx} = \frac{4\pi e^4 z^2 N Z B}{mv^2}, \quad (8)$$

where m is the electronic mass, v is the velocity and ze the charge of the incident particle, N is the number of atoms per cm^3 and Z the nuclear charge of material being traversed, and B is a function only of velocity in a given medium. Comparison of the characteristics of a track from an unknown particle with those of a known particle make track identification possible. The details of emulsion types and compositions, track evaluation, emulsion processing, and auxiliary techniques are covered in review articles by Beiser [1] and Stiller et al. [23].

One of the most versatile emulsions for high-energy particle investigations is the Ilford G.5 type, which is sensitive to all charged particles regardless of their energy. These emulsions are supplied mounted on glass plates in thicknesses from 25 to 1200 microns of any size desired. The thicker emulsions are also supplied as stripped pellicles which can be packed together as a solid block. After exposure they may be separated, mounted on glass plates, and processed. A

stack of pellicles provides a large sensitive volume in which tracks can be followed from one layer to the next, a necessary requirement if detailed analyses of high-energy nuclear events are to be made.

In preparing for this experiment stacks of 28²_{aby}-4-inch 600-micron Ilford G.5 emulsions were used. Two holes were punched into the individual pellicles near the ends. The pellicles were then numbered and assembled between two pieces of 0.25-inch bakelite. The bakelite ends were bolted together by means of close-fitting bolts to insure that there was a known alignment of the pellicles and that they were closely packed. The stack was then wrapped in black paper and tape to make it lighttight during subsequent handling and exposure to the beam. The method used in this experiment for alignment of stripped emulsions is given in a report by Goldhaber et al. [25] .

2. Internal Beam Exposure.

The assembled stack was mounted on a probe head in one of the smaller type air locks shown in Fig. 2a. They were oriented so that the beam particles entered one edge parallel to the plane of the emulsion. The stack was exposed to an integrated proton beam of about 10^7 particles. This resulted in a track density of about 10^5 per cm^2 in the region one inch from the edge that intercepted the greatest portion of the beam. The proton track density has the characteristics of an exponential decay across the plate. If the density is too low, there is only a slight probability of finding interesting events; if it is too high, there are so many tracks that accurate analysis or following of tracks is impossible.

During any exposure it is desirable to determine if the particle flux was of the desired value, to obtain an estimate of background radiation, and to determine effectiveness of shielding if part of stack is to be shielded. To satisfy these requirements test plates (50 or 100 microns thick) are exposed under conditions of geometry similar to the assembled stack before the regular exposure and (or) exposed with the emulsion stack. Test plates (50 microns) can be developed within an hour and a decision made as to whether additional exposure time is required. The small packages taped on the emulsion stack in Fig. 3 show

how test plates were used during a typical exposure of this experiment.

3. Processing Emulsions.

After exposure and before processing, the pellicles were marked by a grid system in order to facilitate the following of tracks through the stack. This was done by contact-printing a numbered grid system of one-millimeter squares upon the bottom of each pellicle. The grid system was oriented with the aid of the alignment holes that had been punched into the pellicles previously. The grid lines and numbers, reproduced by development, were visible when the bottom of the emulsion was brought into the focal plane of a microscope.

After the pellicles were marked, they were mounted on glass plates for processing. The development procedure varies with emulsion thickness. The exact details of chemical solutions, times, temperatures and steps in the development vary somewhat with the quantitative information that one expects to obtain from the emulsions. Some of the requirements influencing the choice of a procedure to be followed are:

- (a) A favorable ratio of track grain density to background grains, so that even the thin tracks of singly charged particles at relativistic velocities can be followed with ease.
- (b) A low level of track distortion, so that reliable multiple Coulomb scattering measurements may be made.
- (c) Uniform development from surface to glass to permit grain density measurements that need not be corrected for track depth in the emulsion.

In this experiment we were concerned with the analysis of particles of relativistic velocities ($g_{\min} \leq g < 1.4 g_{\min}$). A minimum amount of distortion and uniform development were therefore essential. We found that a slight modification of the Bristol development technique gave the most suitable results. The steps, times, and temperatures for this type of development are given in Table II.

Table II

Steps in Bristol Development Method

Stage of Development	Time	Temperature
Presoak	2.5 hours	5° C
Cold developer	2.5 hours	5° C
Dry hot stage	2.25 hours	18° C
Cool for	1 hour	18° to 5° C
Stop bath	2.5 hours	5° C
H ₂ O wash	1 hour	5° C
Fix	54 hours	8° C
Dilution	3 days	8° C
H ₂ O	2 days	5° C
Plasticize	2 hours	5° C
Alcohol dry	60 hours	5° C
Air dry	~24 hours	

CHAPTER V

EXPERIMENTAL METHOD

1. Experimental Nomenclature and Criteria.

In the study of nuclear interactions terms have been defined in different ways by emulsion workers. In the discussion of this experiment the definitions of Camerini et al. [3] are used. These definitions comprise the Bristol notation, which is in general use. Nuclear disintegrations are classified by the number and type of secondary tracks and the type, if known, of the primary particle. Secondary tracks are divided into three classes according to their specific ionization or grain density g . The grain density is compared with the grain density, g_{\min} , of a singly charged particle at minimum ionization. Track classifications are as follows:

- (a) Thin Tracks, $g_{\min} \leq g < 1.4 g_{\min}$ (Represented by n_s)
- (b) Grey tracks, $1.4 g_{\min} < g < 6.8 g_{\min}$ (Represented by N_g)
- (c) Black tracks, $g > 6.8 g_{\min}$ (Represented by N_b)

The thin tracks as defined in (a) are caused by "shower" particles, which are comprised of protons with kinetic energies greater than 500 Mev, pions with kinetic energies greater than 80 Mev, or heavy mesons of intermediate energies. (The number of heavy mesons is very small.) The grey tracks are produced by protons with energies between 25 and 500 Mev. These protons are for the most part due to recoils produced in the early stages of the disintegrations, a process previously discussed in Chapter II. Some grey tracks result from pions of kinetic energy less than 80 Mev, deuterons, and tritons. Pions form less than 5% of the grey tracks [3]. Black tracks are primarily caused by the low-energy evaporation particles, protons, deuterons, tritons, and alpha particles. They are emitted in the final stages of the disintegration.

The sum of the grey and black tracks is designated by N_h , the number of heavy tracks. A star is then characterized by $N_h + n_s$,

followed by a suffix to denote the nature of the particle producing the disintegration (i. e., π for a pion, p for a proton, n for a neutron or an unidentified neutral, and α for alpha particle). For example, a $7 + 2p$ star means that there are seven heavy and two shower tracks originating from a star caused by an incoming proton.

As previously states for stars classified by the Bristol notation, n_s included both pions with kinetic energies greater than 80 Mev and protons with kinetic energies greater than 500 Mev. The number of emitted pions with energies below 80 Mev is small and is equal, in the first approximation, to the number of emitted protons with energies greater than 500 Mev. The value of n_s as observed can therefore be assumed to be an indication of the number of charged mesons emitted. This assumption has been made by cosmic-ray workers [4] and is also made in this experiment. Observations of Fowler et al. [7] at the Cosmotron indicate that few charged mesons are produced with energies below 80 Mev, thus lending further validity to the assumption.

2. Experimental Procedure.

In order to study the results of interactions at known primary energies, stacks of 2-by-4-inch 600-micron Ilford G.5 stripped emulsion pellicles were exposed to the internal beam of the Bevatron at three energies--3.2, 4.8, and 5.7 Mev. Exposures were made on a plunging probe and the modified Bristol development was used. Minimum ionization was determined by grain-counting beam proton tracks, and was found to be 26 grains per 100 microns.

A plate at each energy was selected for this study. The plates were "area-scanned" under 6 x 53 power on a Leitz microscope with an oil-immersion objective lens. Overlapping fields of view were examined to insure complete coverage. Since there is no selective choosing of any particular star size, systematic area scanning gives a representative sample of all stars produced that have two or more prongs. (The efficiency for detection of the one-pronged events is very low unless the plates are scanned along and in the direction of the beam tracks.) Whenever a star was found, it was examined to determine if it was caused by a beam proton. If it was,

the star was then analyzed under 12 x 100 power and classified according to the numbers of heavy and shower tracks. Each track with a specific ionization at or slightly above minimum was tentatively identified as one belonging to a shower particle. Those tracks above minimum were grain-counted to a statistical accuracy of less than 10% and compared with $1.4 g_{\min}$. The identity of the track--as one caused by a heavy particle or a shower particle--was thereby established. Each plate was scanned until 114 primary-beam stars were found.

As a secondary experimental objective, all prongs except the thin tracks were followed to their ends or until they left the plate. Thin tracks were followed for two to three millimeters. The secondary objective was a search for possible interesting events such as double stars (a double star is one in which the incident nucleon has been emitted from another star), hyperon decays, and heavy-meson decays.

CHAPTER VI

EXPERIMENTAL RESULTS

1. Yield Curves for \bar{n}_s and \bar{N}_h .

The average values of the numbers of shower and heavy particles, \bar{n}_s and \bar{N}_h , are plotted on Fig. 4. Each point represents observations on 114 stars, and the indicated error is the standard deviation based on the number of tracks recorded. For comparison, results of Camerini et al. [3] are plotted in dashed lines. Experimental curves show expected increases with primary particle energy. The general shapes are in fair agreement with the results found in cosmic-ray stars, but the values are somewhat lower. For example, at 5.7 Mev experimental values of \bar{n}_s and \bar{N}_h are 1.6 and 11.5; the curves from cosmic-ray stars give values of 2.55 and 13.0.

For that portion of the energy spectrum investigated both yields appear to increase exponentially with the incident nucleon energy. Only a narrow (narrow when compared to the spectrum available in cosmic rays) portion of the primary particle energy spectrum has been used, however, and the statistics are not good enough to make any positive statement in this regard.

The lower \bar{n}_s yield in this experiment might be expected because the cosmic-ray primaries were an admixture of pions and protons. In the center-of-mass system of a nucleon and pion with the nucleon stationary and the pion incident, there is more energy available for meson production than there is in a similar system with an incident proton. This is evident from the expression for the ratio of the amount of energy available for interaction (in the center-of-mass system) with an incoming pion to that available with an incoming proton. If the pion and proton have the same energies, the ratio reduces to

$$\frac{W_{\pi \text{ inc}}}{W_{p \text{ inc}}} \approx \frac{(1 + 2 \gamma_p)^{1/2} - 1}{(2 + 2 \gamma_p)^{1/2} - 2},$$

1

2

3

4

5

6

7

8

9

10

11

12

13

14

15

16

17

18

19

20

21

22

23

24

25

26

27

28

29

30

31

32

33

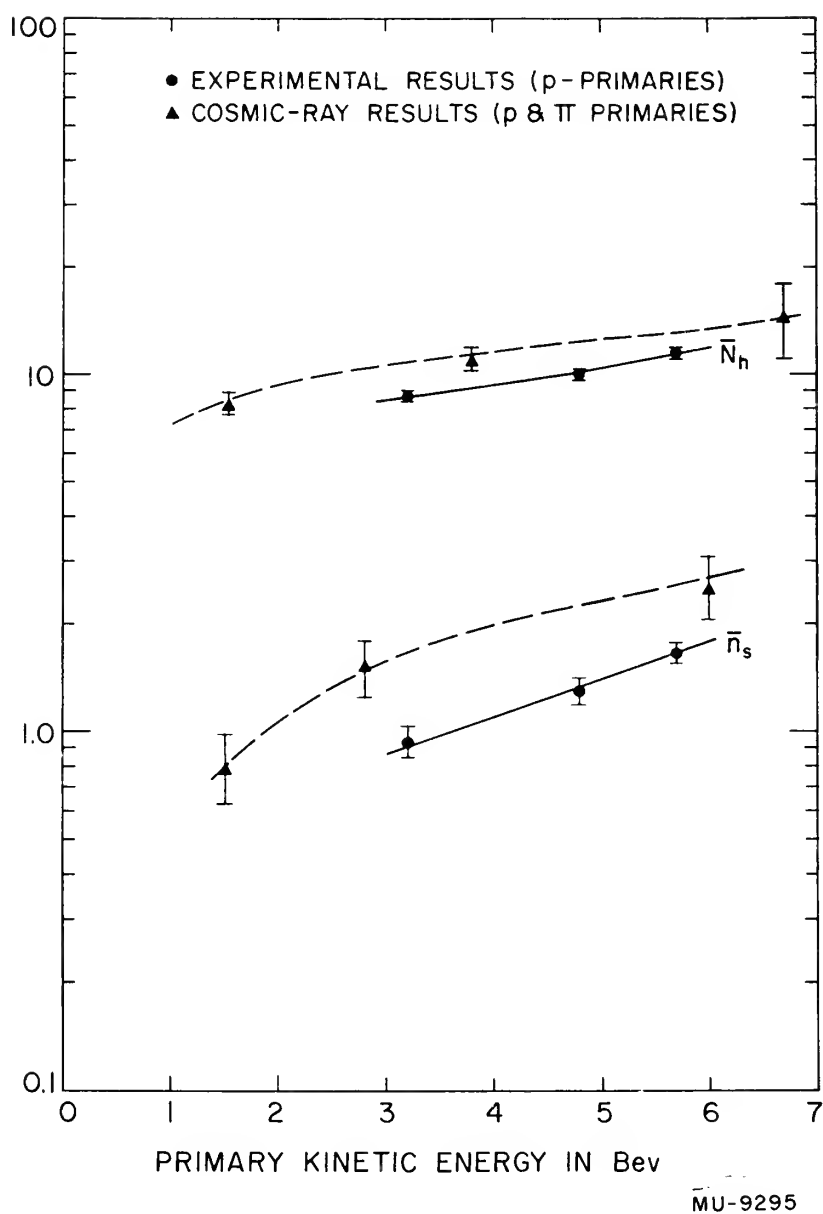


Fig. 4 Comparative plots of the average number of heavy prongs and the average number of shower particles versus kinetic energy of primary particles.

where

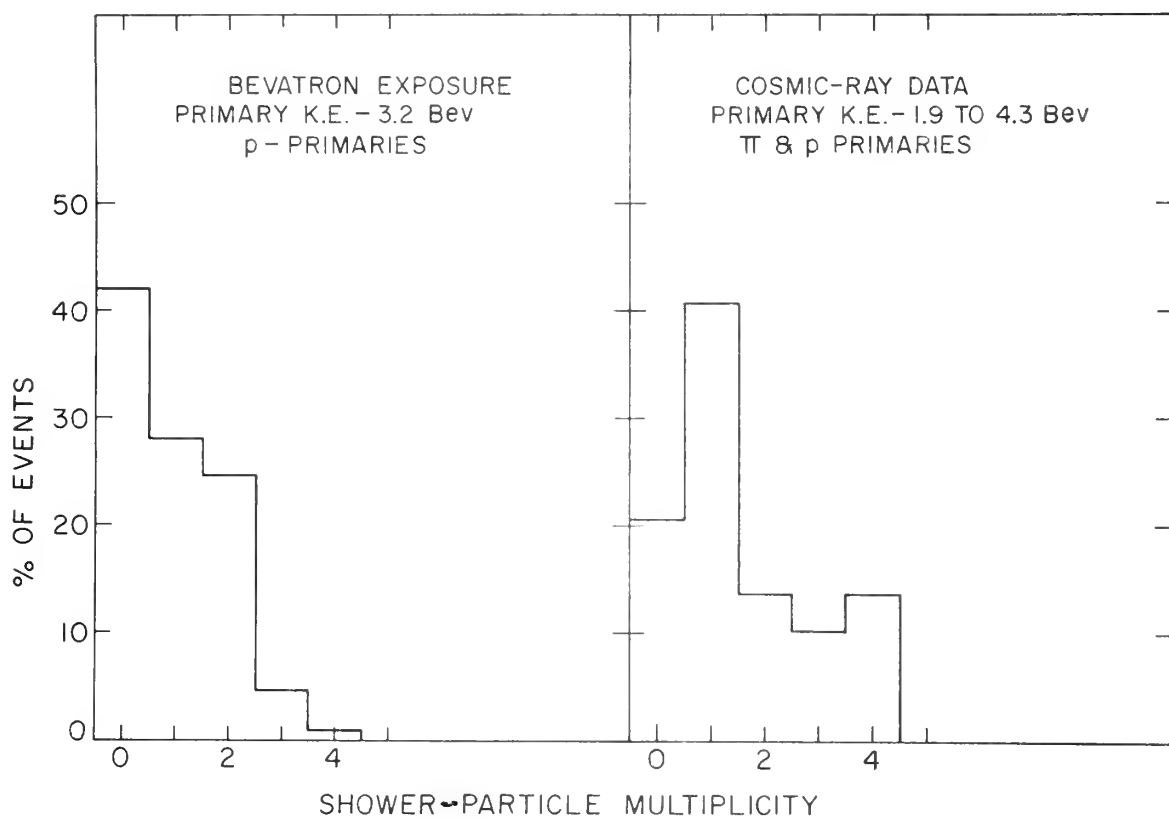
$$\gamma_p = \frac{E_p}{M_p C^2} \quad (9)$$

For a primary energy of 6 Bev the ratio is 1.65. From the experimental curve for incident protons \bar{n}_s is found to be 1.8 at 6 Bev. If cosmic rays were assumed to contain 50% pions, \bar{n}_s would equal $(1.8/2)(1 + 1.65)$ or 2.4. At 6 Bev, curves of shower-particle production in stars produced by cosmic rays at 11,000 feet show \bar{n}_s to be 2.5.

A second possible contribution to the difference between the two observations may be in the measurement of the primary particle energy. In this experiment the energy of the Bevatron beam is well known, but cosmic-ray primary energies have been determined by multiple-scattering measurements and are subject to error. From a discussion of this point with cosmic-ray workers [21] I was advised that they feel that their energy measurements are accurate within five percent in the energy region below 10 Bev. From this it can be concluded that differences must be caused by the pions among the cosmic-ray primaries. The exact pion contribution cannot be readily determined.

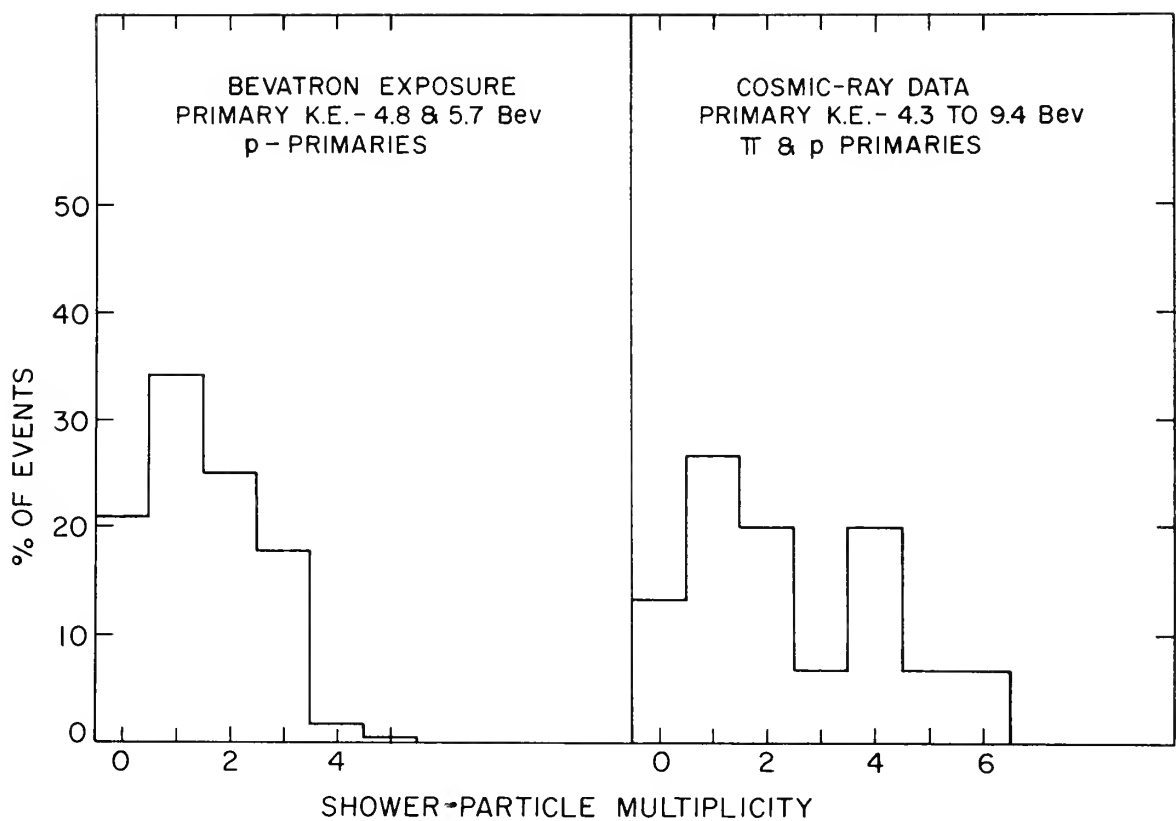
2. Shower-particle Multiplicity.

The first conclusion stated in the previous section is further substantiated by the plots in Figs. 5 and 6. These plots represent the observed multiplicities rather than the average values discussed previously. Figure 5 contains comparative normalized plots of the shower-particle multiplicity as observed for cosmic-ray primaries [3] in the energy range of 1.9 to 4.3 Bev and the multiplicity as observed experimentally at 3.2 Bev. Figure 6 shows the same observations at cosmic-ray energies between 4.3 and 9.4 Bev and at energies of 4.8 and 5.7 Bev in this experiment. These plots are not exact comparisons since the observations in this experiment were made at specific known energies and the cosmic-ray observations covered a relatively wide band. The experimental energies, however, represent fair medians of the cosmic-ray energy bands. The proportion of stars



MU-9296

Fig. 5. Comparative normalized distributions of number of events versus shower-particle multiplicity.



MU-9297

Fig. 6. Comparative normalized distributions of number of events versus shower-particle multiplicity.

1. The first part of the report is a general
 introduction to the subject of the study.
 2. The second part is a detailed description of the
 methods used in the study.

100

104

TWENTY-THREE
 100

10

100

100

The following table shows the results of the study.
 The first column shows the number of subjects in each group.
 The second column shows the mean score for each group.
 The third column shows the standard deviation for each group.

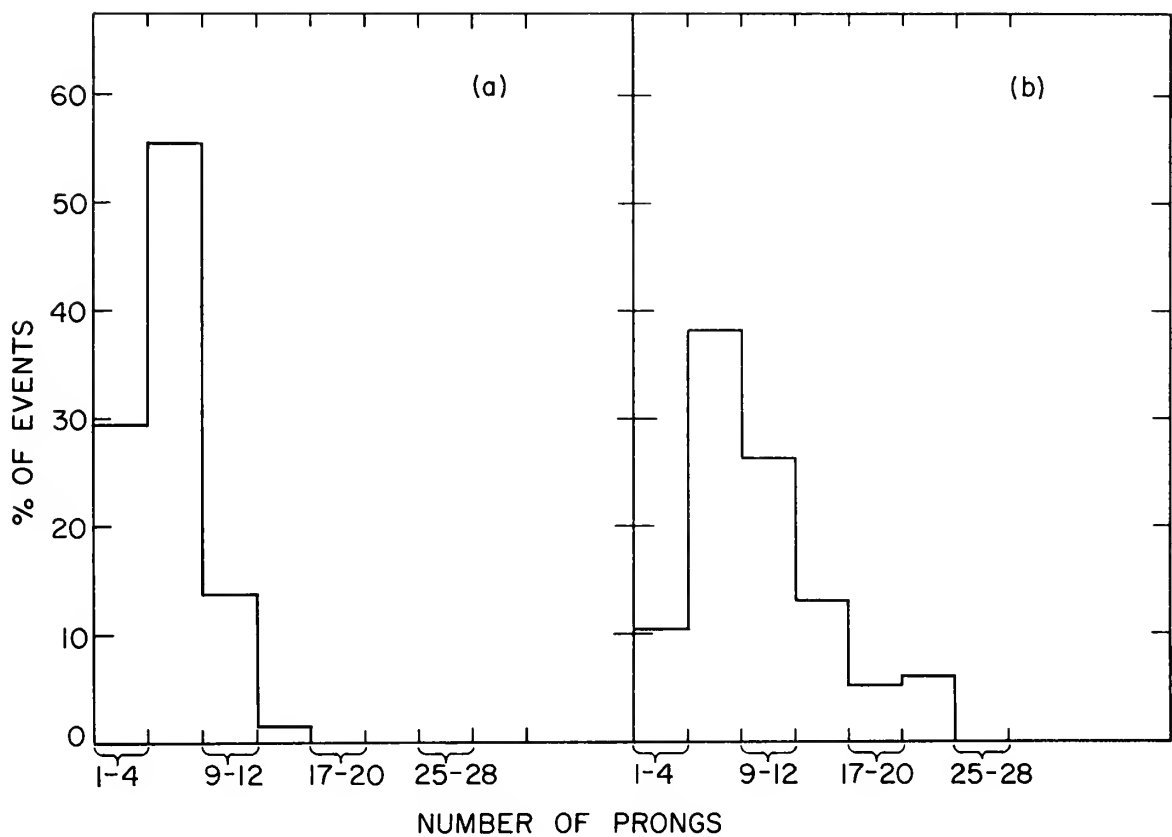
with n_s equal to zero is greater by a significant amount in each case with "p" primaries (this experiment) than with " π and p" primaries (cosmic-ray observations). This then, is additional evidence that in the mechanism of individual collisions within the atomic nuclei a meson is more effective than a nucleon of the same energy in producing additional mesons.

The two figures indicate another feature of meson production-- the wide spread in multiplicity at any given primary energy. This would be expected from the statistical nature of meson production, and indicates very definitely that shower-particle multiplicity in an individual event is an unreliable indication of primary particle energy in the portion of the incident energy spectrum investigated. With extremely high-energy cosmic-ray primaries upwards of 30 mesons are produced. In these collisions the number of mesons is used to estimate the primary energy.

3. Distribution of Star Sizes.

Figures 7b - 7d are normalized histograms of the number of events with N prongs versus the number of prongs at the primary energies of this experiment. Figure 7a is a similar plot of data at 1 Bev found by Lock et al. [20] at Birmingham. (The Birmingham data have been included as additional information on how the general shape of the prong distribution changes with primary energy.) An interval of four prongs has been used on the abscissa in order to reduce the statistical fluctuations that would result from the small number of stars used for this analysis.

The histograms show peaks in the 4- to 8-prong interval. This range represents the maximum number of prongs from the complete breakup of the light nuclei of the emulsion; i. e., carbon nitrogen, and oxygen. The numerical value at the maximum decreases with increasing energy. The change in distribution results from the presence of more stars with greater numbers of prongs. These larger stars are due to the more complete breakup of the heavier nuclei, silver and bromine. The increase in the number of mesons produced



MU-9298

Fig. 7a. Normalized histogram of number of events with N prongs versus number of prongs. Primary energy 1.0-Bev. From data of Lock et al. [20].

7b. Primary energy 3.2-Bev.

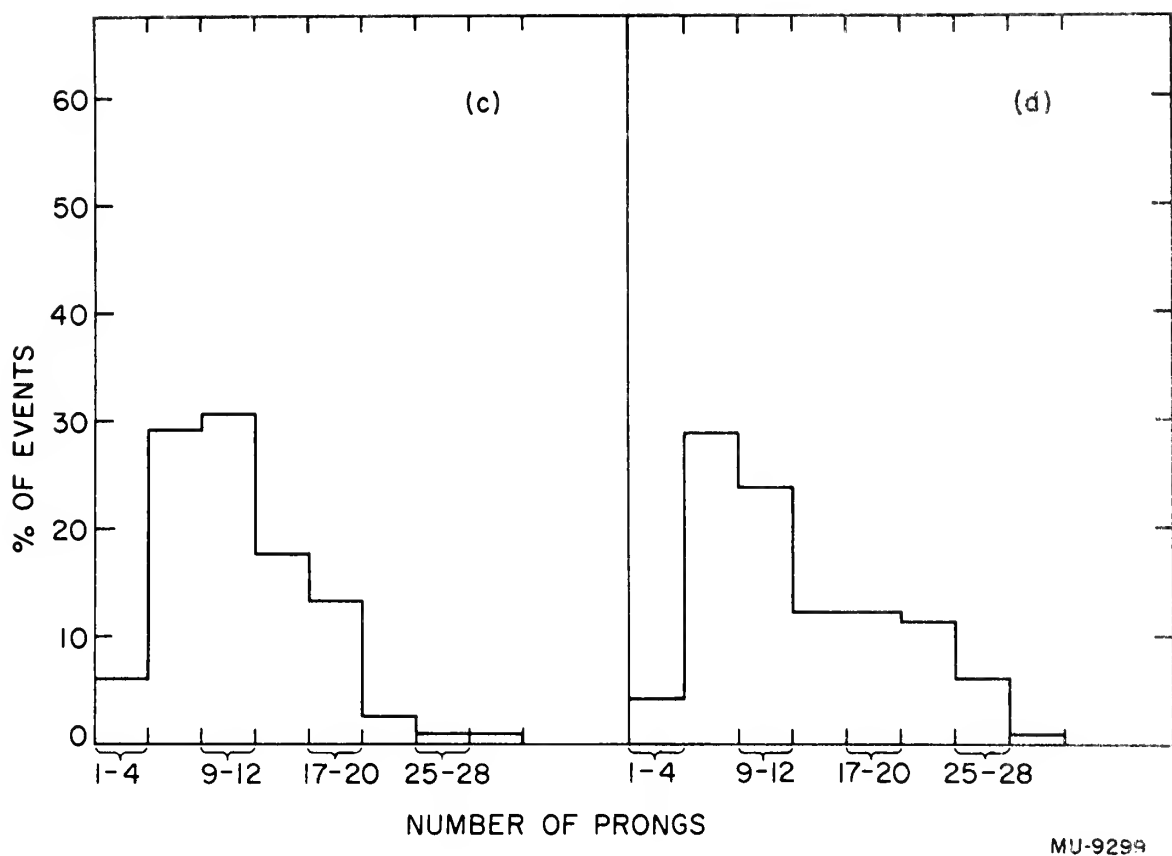


Fig. 7c. Normalized histogram of number of events with N prongs versus number of prongs. Primary energy 4.8-Bev.
7d. Primary energy 5.7-Bev.

21M3V3 30.0°

contributes negligibly to the larger stars because of the small change in multiplicity. The peak is broadened on the side towards the greater number of prongs and there is a slight indication that a second peak is developing in the 17- to 20-prong interval at 5.7 Bev. This peak might become apparent if the investigation were extended to higher primary energies. With good statistics and higher primary energies, it is a reasonable assumption that one will be able to see definite peaks representing the breakup of the atoms of different mass number. The increase in star size with primary energy can be seen in Table III.

Table III

Average Number of Prongs per Star

Primary Energy in Bev	Average Number of Prongs
1.0 (a)	5.7
3.2	9.6
4.8	11.3
5.7	13.1

a The data of Lock et al. [20] include one-prong stars, but they have been excluded in this computation of averages because no one-prong stars were recorded in this experiment. Lock's one-prong stars were found for the most part by scanning along the track (Chap. V, Sect. 2).

4. Comparison of Disintegrations of Light and Heavy Nuclei.

A comparison of the average multiplicity of n_s with N_h is also of interest in order to observe any effect that nuclear size might have on shower-particle production. Stars with N_h greater than eight must generally result from the disintegration of the silver and bromine nuclei, while smaller stars can be due to both the light and heavy nuclei within the emulsion. The exact proportional contributions from the heavy and light elements to stars with $N_h \geq 9$ cannot be easily

determined because of the statistical processes involved and the variation in the thermal excitation energy available after the collision. The energy available varies with the number of mesons produced and the number of particles that escape before evaporation starts.

Figure 8 is a plot of average multiplicity as a function of the primary energy for two classes of stars, $4 \leq N_h < 9$ and $N_h \geq 9$. Cosmic-ray observations in this energy range are included for comparison. There is no significant difference between the two classes of stars; the curve for the stars with $4 \leq N_h < 9$ shows a slightly greater multiplicity, but the standard deviations of all points on both curves overlap about 50 %. Cosmic-ray workers [4] had overlapping points below 10 Bev without a definite trend in either set of points, but they noted that \bar{n}_s was greater for the heavy nuclei at 14 Bev -- 4.3 for heavy nuclei and 2.4 for light.

Figure 9 is a plot similar to Fig. 8, but only those events in which the shower-particle multiplicity was equal to or greater than unity are included. There is no significant difference between the two plots, and the same comments apply. Figure 8 undoubtedly included events in which only uncharged pion (s) were produced. These events would be excluded for the most part in Fig. 9, and one would expect differences in the two curves only if there were a significant difference in the numbers of charged and neutral mesons produced.

It may be possible that secondary generation would be more evident in heavy nuclei, because of the greater number of mean free paths to be traversed before escape, and would thereby cause the shower-particle multiplicity to be increased in these stars. On the other hand, reabsorption of mesons in the parent heavy nucleus will tend to reduce the number of emitted mesons and increase the number of recoiling nucleons. It is reasonable to assume that this reabsorption is the more important process in the energy range of this experiment, and the secondary generation process gains in importance at energies greater than 10 Bev. Reabsorption may explain stars that have a large value for N_h but a small n_s when compared with their

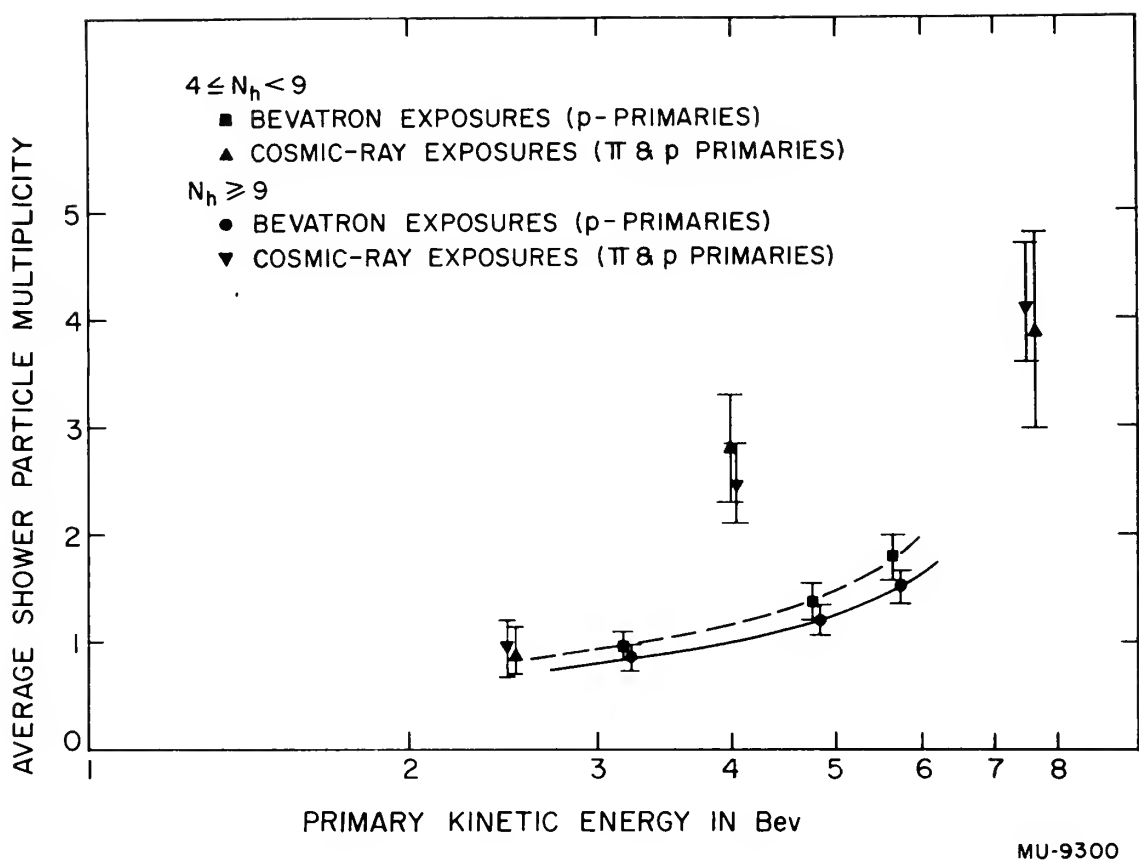
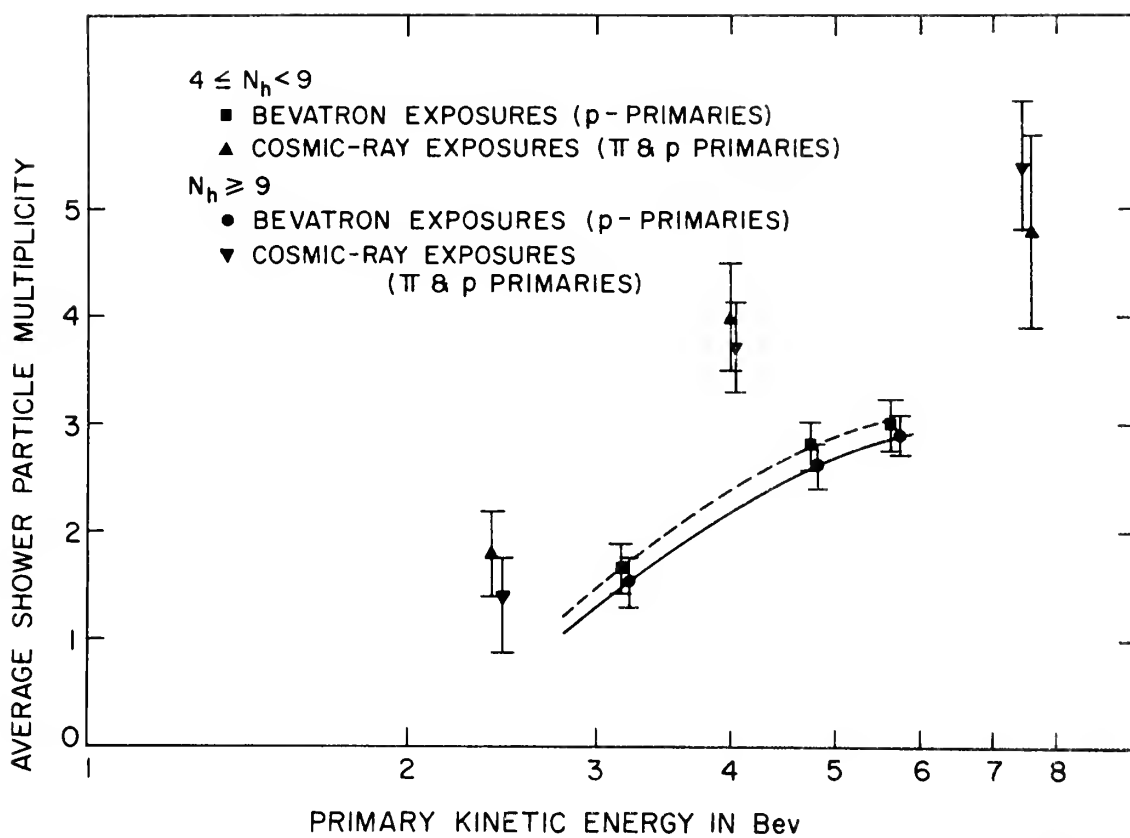


Fig. 8. Variation of average shower particle multiplicity per event versus kinetic energy of primary in BeV. ($n_s \geq 0$)



Figure 1. Analysis of the data. The plot shows the relationship between X and Y. The dashed line represents the linear regression fit.



MU-9301

Fig. 9. Variation of average shower particle multiplicity per event versus kinetic energy of primary in BeV. ($n_s \geq 1$)

1 2 3 4 5 6 7 8 9 10 11 12

ВВЕДЕНИЕ
 Глава I. Арифметика
 Глава II. Алгебра
 Глава III. Геометрия
 Глава IV. Тригонометрия
 Глава V. Начала высшей математики

respective average values.

5. General Observations.

It is interesting to note some qualitative general observations made during this study. These observations concern angular distributions and secondary experimental objectives.

The shower particles were strongly concentrated in the beam direction. Occasionally a track from a star in which there was multiple production would extend in the backward direction. The latter tracks were not collimated parallel to the beam direction to the same degree as were the former.

There was, in general, an isotropic distribution of the black tracks, but in several stars with more than fifteen tracks there were three or more black tracks that almost overlapped. It appeared that one section of the nucleus had gained momentum in a certain direction and that this fragment broke into more elementary particles as it left the nucleus. This phenomenon was exhibited at two or three points in the largest stars, and might be considered to be due to some kind of local heating. Fujimoto and Yamaguchi [8, 9], in their discussions of nuclear evaporation, consider local heating to be extremely rare, but their predictions did not include the potentially high energies available within a nucleus penetrated by 6 Bev protons. Similar phenomena have been reported in cosmic-ray stars [11].

In the search for interesting events by following prongs, eleven double stars were found, and seven low-energy pions were seen ending and forming σ -stars. No positive-pion, heavy-meson, or hyperon decays were noted that could be positively identified. With regard to the pions, these results support the statements of Brown et al. [2], who found that 95% of the slow mesons produced in stars are negatively charged. This result can be attributed to the effect of nuclear charge, which will cause positive particles to be emitted with greater kinetic energy than negative ones. Therefore they will escape from the emulsion except in rare cases.

6.

xiv

76

W. H.

.. 23

1911

3.10

WILEY

211

117

10

20

۲۱

50

62

21

100

6

3

 λ_1

1

1.1.3

54

CHAPTER VII

THEORETICAL COMPARISONS

1. Fermi Model.

Fermi used his statistical model to calculate meson production at Cosmotron energies. His calculations have been extended to compute the expected meson production at the beam energies of this experiment. The complete calculations have been carried out for proton-neutron (p-n) and proton-proton (p-p) collisions at each energy. Details of the calculations are similar to those described in Fermi's papers [5,6], discussed in Chapter II. An assumption is made in tabulating expected probabilities that there is a like number of p-n and p-p collisions. The final results of the calculations, together with experimental observations, have been summarized in Table IV.

The Fermi statistical model shows fair agreement for average production, but the rate of increase with energy is lower. This could be accounted for in part by the restriction, $n_s \leq 3$, in the calculations. The observations at 5.7 Bev include five stars with $n_s > 3$. Exclusion of these events would reduce the observed multiplicity to 1.46 ± 0.12 , which compares favorably with the computed 1.44. There is less agreement in the actual percentages of stars with the various values of n_s , but general shapes of the distributions are comparable.

2. Lepore Model.

Lepore made some changes to the Fermi model in postulating his model [18]. He has made calculations to determine the expected production at 2.5, 3.9, and 4.71 Bev (center-of-mass system). In the laboratory system of two colliding nucleons, one of which is at rest, 6.3 Bev is equivalent to 3.9 Bev in the center-of-mass system.

Table IV
Observed and Calculated Shower-Particle
Multiplicity Percentages--Fermi Model

Energy in Bev	n_s	Extension of Fermi's Calculations ^a	Experimental Observations
3.2	0	20	42
	1	47	28
	2	29	25
	3	4	4
	4	--	1
	Av. $\frac{4}{n_s}$	1.17	0.94 ± 0.09
5.7	0	16	25
	1	41.5	38
	2	35	20
	3	7.5	17
	4	--	0
	Av. $\frac{4}{n_s}$	1.34	1.3 ± 0.11
5.7	0	14	17
	1	38	31
	2	38	30
	3	10	18
	4	--	3
	Av. $\frac{5}{n_s}$	1.44	1.62 ± 0.11

- a In the computation of the percentages for each value of n_s the tabulated number represents the shower tracks that would actually be observed, not the number of pions created. The numbers in column 3 for $n_s = 2$ include the following production schemes: $pp + -$, $nn ++$, $pp + - 0$, $nn ++ 0$, and $pn + - 0$. (The +, - and 0 refer to the charge of the created mesons.)

Energy		Energy		Energy	
10	10	10	10	10	10
20	20	20	20	20	20
30	30	30	30	30	30
40	40	40	40	40	40
50	50	50	50	50	50
60	60	60	60	60	60
70	70	70	70	70	70
80	80	80	80	80	80
90	90	90	90	90	90
100	100	100	100	100	100
110	110	110	110	110	110
120	120	120	120	120	120
130	130	130	130	130	130
140	140	140	140	140	140
150	150	150	150	150	150
160	160	160	160	160	160
170	170	170	170	170	170
180	180	180	180	180	180
190	190	190	190	190	190
200	200	200	200	200	200
210	210	210	210	210	210
220	220	220	220	220	220
230	230	230	230	230	230
240	240	240	240	240	240
250	250	250	250	250	250
260	260	260	260	260	260
270	270	270	270	270	270
280	280	280	280	280	280
290	290	290	290	290	290
300	300	300	300	300	300
310	310	310	310	310	310
320	320	320	320	320	320
330	330	330	330	330	330
340	340	340	340	340	340
350	350	350	350	350	350
360	360	360	360	360	360
370	370	370	370	370	370
380	380	380	380	380	380
390	390	390	390	390	390
400	400	400	400	400	400
410	410	410	410	410	410
420	420	420	420	420	420
430	430	430	430	430	430
440	440	440	440	440	440
450	450	450	450	450	450
460	460	460	460	460	460
470	470	470	470	470	470
480	480	480	480	480	480
490	490	490	490	490	490
500	500	500	500	500	500
510	510	510	510	510	510
520	520	520	520	520	520
530	530	530	530	530	530
540	540	540	540	540	540
550	550	550	550	550	550
560	560	560	560	560	560
570	570	570	570	570	570
580	580	580	580	580	580
590	590	590	590	590	590
600	600	600	600	600	600
610	610	610	610	610	610
620	620	620	620	620	620
630	630	630	630	630	630
640	640	640	640	640	640
650	650	650	650	650	650
660	660	660	660	660	660
670	670	670	670	670	670
680	680	680	680	680	680
690	690	690	690	690	690
700	700	700	700	700	700
710	710	710	710	710	710
720	720	720	720	720	720
730	730	730	730	730	730
740	740	740	740	740	740
750	750	750	750	750	750
760	760	760	760	760	760
770	770	770	770	770	770
780	780	780	780	780	780
790	790	790	790	790	790
800	800	800	800	800	800
810	810	810	810	810	810
820	820	820	820	820	820
830	830	830	830	830	830
840	840	840	840	840	840
850	850	850	850	850	850
860	860	860	860	860	860
870	870	870	870	870	870
880	880	880	880	880	880
890	890	890	890	890	890
900	900	900	900	900	900
910	910	910	910	910	910
920	920	920	920	920	920
930	930	930	930	930	930
940	940	940	940	940	940
950	950	950	950	950	950
960	960	960	960	960	960
970	970	970	970	970	970
980	980	980	980	980	980
990	990	990	990	990	990
1000	1000	1000	1000	1000	1000

The following table shows the results of the experiments conducted on the 10th of May 1900. The experiments were conducted on the 10th of May 1900. The results of the experiments are shown in the following table.

Table V is a summary of the expected pion production at this energy from Lepore's paper.

Table V
Pion Production at 6.3 Bev--Lepore Model

Pions Produced	Lepore's Calculations for 6.3 Bev	Observed n_s Percentage at 5.7 Bev
0	12	17
1	38	31
2	40	30
3	10	18
4	--	3
5	--	1
Average	1.48	1.62 ± 0.11

Lepore's computations were for indistinguishable particles; therefore the figures in column 2 of Table V include positive, negative, and neutral pions. When equal distributions of the three types of pions are assumed, tracks from only two-thirds of the particles could be observed in emulsions. The observable average would be 1.0, which is to be compared with 1.9 from the experimental curve at 6.3 Bev.

3. Other Theories.

The other theories of meson production discussed in Chapter II do not yield easily to calculation in the energy range of this experiment. Average multiplicities from the theories of Heitler and Heisenberg have been plotted by Camerini et al. [4]. Table VI contains the values obtained from these curves.

Table VI

Average Shower-Particle Multiplicities;
Heitler and Heisenberg Theories

Primary Kinetic Energy in Bev	Average shower-particle multiplicity, \bar{n}_s				
	Heitler Theory	Heisenberg Theory a			Observed
		K = 1.0	K = 0.7	K = 0.3	
3.2	2.0	2.1	1.7	0.9	0.94
4.8	2.9	2.6	1.9	1.1	1.3
5.7	3.1	3.0	2.1	1.2	1.62

a K is the degree of inelasticity of the collision. A completely elastic collision is denoted by $K = 0$.

The plural theory of Heitler gives values that are high compared with the observations. The data derived from Heisenberg's theory appear to be in fair agreement with the experimental results if the K-value is near 0.4. It is also interesting to note that the Heisenberg theory postulates multiple production, as does the Fermi theory. There is not sufficient information in the theories to determine and compare the predicted percentage distributions of the particles, as could be done with the Fermi and Lepore theories.

4. General Comment.

The experimental results and the discussion of the various theoretical approaches to the problem of meson production indicate that there are many questions to be answered in this field. More pion-nucleon and nucleon-nucleon experiments conducted in the 1- to-10-Bev energy range would shed much light on the problem. This experiment appears to give some evidence of the correctness of one phase of the Fermi theory, but more definite conclusions must await experimental data with better statistics and a more complete and detailed analysis of all the products of nuclear disintegrations. The analysis needs to include the identification and the energy spectrum of all products, the directions of emission, the charge distributions, and the identification of target nuclei. Only the joint efforts of many experimenters for an extended time may furnish the answers.

BIBLIOGRAPHY

1. Beiser, A. NUCLEAR EMULSION TECHNIQUE
Revs., Modern Phys., Vol. 24,
No. 4, pp 272-310, October 1952

2. Brown, R.H., Camerini,
V., Fowler, P.H. Heitler,
H., King, D.T., and
Powell, C.F. NUCLEAR TRANSMUTATIONS
PRODUCED BY COSMIC RAY
PARTICLES OF GREAT ENERGY
Part I. OBSERVATIONS WITH
PHOTOGRAPHIC PLATES EX-
POSED AT AN ALTITUDE OF
11,000 FT.
Phil. Mag., Vol. 40, Ser. 7
pp 862-881, August 1949

3. Camerini, V., Davies,
J.H., Fowler, P.H.
Franzinetti, C., Muirhead,
H., Lock, W.O., Perkins,
D.H., and Yekutielli, C. NUCLEAR TRANSMUTATIONS
PRODUCED BY COSMIC RAY
PARTICLES OF GREAT ENERGY
Part VI. EXPERIMENTAL
RESULTS ON MESON PRODUCTION
Phil. Mag., Vol. 42, Ser. 7
pp 1241-1260, November 1951

4. Camerini, V., Davies,
J.H. Franzinetti, C.,
Lock, W.O., Perkins,
D.H., and Yekutielli, C. NUCLEAR TRANSMUTATIONS
PRODUCED BY COSMIC RAY
PARTICLES OF GREAT ENERGY
Part VII. INTERPRETATION OF
THE EXPERIMENTAL RESULTS
Phil. Mag., Vol. 42, Ser. 7
pp 1261-1276, November 1951

5. Fermi, E. HIGH ENERGY NUCLEAR EVENTS
Prog. Theor. Phys., Vol. 5,
No. 4 pp 570-583, July-August
1950

6. Fermi, E. MULTIPLE PRODUCTION OF
PIONS IN NUCLEON-NUCLEON
COLLISIONS AT COSMOTRON
ENERGIES
Phys. Rev., Vol. 92, No. 2
pp 452-453, October 1953;
Errata Phys. Rev. Vol. 93, No. 6
pp 1434-1435, March 1954

7. Fowler, W.B., Shutt,
R.P., Thorndike, A.M.,
and Whittemore, W.L. MESON PRODUCTION IN N-P
COLLISIONS AT COSMOTRON
ENERGIES
Phys. Rev., Vol. 95, No. 4
pp 1026-1044, August 1954

8. Fujimoto, Y. and Yamaguchi, Y. ON THE NUCLEAR STARS
Prog. Theor. Phys., Vol. IV, No. 4
4 October-December 1949
9. Fujimoto, Y. and Yamaguchi, Y. HIGH ENERGY NUCLEAR EVAPORATION
Prog. Theor. Phys., Vol. V, No. 5
pp 787-799, September-October 1950
10. Harding, J. B. CROSS SECTION FOR NUCLEAR DISINTEGRATIONS PRODUCED BY COSMIC RAYS
Nature, Vol. 163, No. 4142, pp 440-441, March 1949
11. Harding, J. B., Lattimore, S., and Perkins, D. H. NUCLEAR DISINTEGRATIONS PRODUCED BY COSMIC RAYS
Proc. Roy. Soc., (London), Vol. A196, pp 325-343, April 1949
12. Heisenberg, W. PRODUCTION OF MESON SHOWERS
Nature, Vol. 164, No. 4158, pp 65-66, July 1949
13. Heitler, W. THEORY OF MESON PRODUCTION
Revs. Modern Phys., Vol. 21, No. 1 pp 113-121, January 1949
14. Heitler, W. and Janossy, L. ON THE SIZE-FREQUENCY DISTRIBUTION OF PENETRATING SHOWERS
Proc. Phys. Soc., Vol. A62, Part II pp 669-683, November 1949
FURTHER INVESTIGATION ON THE PLURAL PRODUCTION OF MESON SHOWERS
Helv. Phys. Acta, Vol. 23, No. 4 pp 417-431, 1950
15. Kerst, D. W. ACCELERATION OF ELECTRONS BY MAGNETIC INDUCTION
Phys. Rev., Vol. 60, No. 1 pp 47-53, July 1941
16. Kerst, D. W. and Serber, R. ELECTRONIC ORBITS IN THE INDUCTION ACCELERATOR
Phys. Rev., Vol. 60, No. 1 pp 53-58, July 1941

17. LeCouteur, K. J. THE EVAPORATION THEORY OF
NUCLEAR DISINTEGRATIONS
Proc. Phys. Soc. (London), Vol. 63,
Part 3, pp 259-282, 1 March 1950

18. LePore, J. V. and NUCLEAR EVENTS AT HIGH
Stuart, R. N. ENERGIES
Phys. Rev., Vol. 94, No. 6
pp 1724-1727, June 1954

19. Lewis, H. W. THE MULTIPLE PRODUCTION OF
Oppenheimer, J. R., and MESONS
Wouthuysen, J. A. Phys. Rev., Vol. 73, No. 2
pp 127-140, January 1948

20. Lock, W. O., March, NUCLEAR INTERACTIONS OF
P. V., Muirhead, H., and 1000-MEV PROTONS IN NUCLEAR
Rosser, W. G. V. EMULSIONS
to be published in Proc. Royal
Society

21. Menon, N. G. K. Private communication

22. Milburn, R. H. STATISTICAL THEORY OF
MULTIPLE MESON PRODUCTION
Revs. Modern Phys., Vol. 27,
No. 1, pp 1-14, January 1955

23. Stiller, B., Shapiro, TECHNIQUE FOR PROCESSING
M. M. and O'Dell, F. W. THICK NUCLEAR EMULSIONS
Rev. Sci, Instr. Vol. 25, No. 4,
pp 340-348, April 1954

24. Bohm, D. and Foldy, L. THEORY OF THE SYNCHROTRON
Phys. Rev., Vol. 70, No. 5
pp 249-258, September 1946

25. Goldhaber, G., Goldsack, METHOD FOR ALIGNMENT OF
S. J., and Lannutti, J. E. STRIPPED NUCLEAR EMULSIONS
UCRL-2928, pp 1-11 March 23,
1955



Thesis
J65

28457

Johnson
Multiple meson
production in emulsions
exposed to the bevatron
beam.

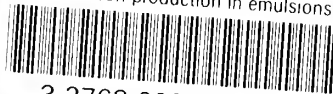
Thesis
J65

28457

Johnson
Multiple meson production
in emulsions exposed to the
bevatron beam.

thes.J65

Multiple meson production in emulsions e



3 2768 002 10556 1

DUDLEY KNOX LIBRARY